MINISTRY OF HIGHER EDUCATION AND SCIENTIFIC RESEARCH

UNIVERSITY FELIX HOUPHOUET BOIGNY

TRAINING AND RESEARCH UNIT FOR STRUCTURE SCIENCES OF MATTER AND TECHNOLOGY

REPUBLIC OF CÔTE D'IVOIRE
UNION - DISCIPLINE - TRAVAIL

DEPARTMENT OF PROCESS METALLURGY AND METAL RECYCLING OF RWTH AACHEN UNIVERSITY

N°825

SPONSORED BY THE Federal Ministry of Education and Research

INTERNATIONAL MASTER PROGRAM

IN ENERGY AND GREEN HYDROGEN

SPECIALITY: GREEN HYDROGEN PRODUCTION AND THECHNOLOGY

MASTER THESIS

Topic:

Synthesis of Copper, Silver, and Copper–Silver Powders via Ultrasonic Spray Pyrolysis and Hydrogen Reduction

Presented on 23 of September 2025 by:
FAYE, Mame Haicha

Jury:

Professor OBROU Kouadio Olivier	President
Dr (MC) ESSY Kouadio Fodjo	Examiner
Dr. KONE Daouda	Main supervisor
Dr. Srećko Stopic	Co-supervisor

ACADEMIC YEAR 2023/2025

DEDICATION

I dedicate this thesis to the memory of my beloved father Saliou FAYE, who was an exceptional father and role model to me. He believed in the power of education and made countless sacrifices to put me in school, paving the way for every diploma I have earned up to this stage. His wisdom, love, and guidance continue to inspire me every day, and this achievement stands as a testimony to his vision and efforts for my future.

I would also like to dedicate this work to my mother, Alice BAMPOKY, for her love and prayers. To my sisters, Amina Marie FAYE and Adja Rokhaya FAYE, thank you for your support and encouragement.

This success also belongs to all my family for their love and patience.

ACKNOWLEDGEMENTS

First and foremost, I thank God for granting me strength, health, and perseverance throughout this journey. Without His guidance and blessings, none of this work would have been possible.

I would like to express my deepest gratitude to WASCAL and the German Federal Ministry of Education and Research (BMBF) for their generous support throughout my academic path. My sincere appreciation goes the Vice Chancellor of Félix Houphouët-Boigny University, for extending the same warm hospitality and support during the second year of the program in Abidjan, Côte d'Ivoire. My heartfelt thanks also go to Prof. Edouard KOUASSI, Director of WASCAL–Côte d'Ivoire, for the invaluable material and logistical support provided during the second year of my Master's studies. I am equally thankful to the President of Abdou Moumouni University, for hosting and providing excellent facilities during the first year of the Master program in Niamey, Niger. I am especially grateful to Prof. Bernd Friedrich, Head of IME at RWTH Aachen University, for granting me unrestricted laboratory access and abundant resources that greatly enriched my research experience. I would like to sincerely acknowledge the constant guidance and support of my supervisor, Dr. Daouda KONE, whose availability and constructive feedback were essential in shaping this thesis. My deep gratitude also goes to my co-supervisor, Dr. Srećko Stopic, for his unwavering guidance, insightful advice, and confidence in my abilities, which motivated me to give the best of myself. I also extend warm thanks to his collaborator, Dusko Kostić, for his invaluable assistance during my experiments. I am also honored to acknowledge the members of my defense jury: Professor OBROU Kouadio Olivier, President of the Jury, and Dr (MC) ESSY Kouadio Fodjo, Examiner, for taking the time to review my work and provide their valuable feedback.

Finally, I would like to thank all the administrative staff of WASCAL and IMP–EGH (Julich and Aachen) for their dedicated efforts in organizing the program and coordinating enriching workshops and educational events. Special thanks are due to Majid Is-Hak, Nar Ndiaye, and Ndeye Ngone Sarr for their kind support during the final stages of this work, particularly during the reduction of my thesis.

Abstract

This thesis investigates the synthesis of copper (Cu), silver (Ag), and copper–silver (Cu-Ag) powders via ultrasonic spray pyrolysis (USP) and hydrogen reduction, focusing on how gas atmosphere, reduction temperature, and precursor ratio affect their morphology, particle size, purity, and stability. Understanding these parameters is important because they control how nanoparticles form, which affects their conductivity, catalytic activity, and resistance to oxidation. These properties are very important for many uses, such as making conductive inks and printed circuits for electronics, catalysts for chemical and energy processes, and protective coatings that stop corrosion or kill germs. In this work, four solutions were made using copper nitrate trihydrate and silver nitrate, then sprayed in a USP reactor and reduced under hydrogen and argon at temperatures between 500 °C and 700 °C. The powders made were studied with SEM and ImageJ to see their size and shape, and EDS to check their composition. The results show that the gas atmosphere had a strong effect on the particle size and shape. Hydrogen made particles more pure but also bigger and less uniform for silver, while argon gave more and smaller particles that looked more similar. For copper, using 600 °C and 650 °C made even smaller ones but with more clumping, which could help in catalytic use. For the Cu-Ag powders, the ratio of the two metals affected how stable the powders were: a 1:1 ratio gave small, uniform, core-shell particles without oxidation, while a 1:3 ratio caused clumping and surface oxidation. This work shows that gas type, temperature, and metal ratio are key to controlling the final powders with tunable surfaces and better stability.

Key words: Ultrasonic Spray Pyrolysis; Hydrogen Reduction; Nanoparticles; Bimetallic powders; Gas atmosphere; Precursor ratio; Reduction temperature.

Résumé

Cette thèse étudie la synthèse de poudres de cuivre (Cu), d'argent (Ag) et de cuivre-argent (Cu-Ag) par pyrolyse par pulvérisation ultrasonique (USP) suivie d'une réduction à l'hydrogène, en se concentrant sur l'influence de l'atmosphère gazeuse, de la température de réduction et du rapport précurseur sur leur morphologie, taille de particules, pureté et stabilité. Comprendre ces paramètres est essentielle car ils déterminent la formation des nanoparticules et influence directement leur conductivité, leur activité catalytique et leur résistance à l'oxydation. Ces caractéristiques sont cruciales pour des applications telles que les encres conductrices et circuits imprimés, les catalyseurs pour réactions chimiques et systèmes énergétiques, ainsi que les revêtements durables anticorrosion ou antimicrobiens. Quatre solutions précurseurs ont été préparées à partir de nitrate de cuivre trihydraté et de nitrate d'argent, puis pulvérisées dans un réacteur et réduites sous atmosphère d'hydrogène et d'argon à des températures entre 550 °C et 700 °C. Les poudres obtenues ont été analysées par MEB (Microscopie électronique a balayage) et ImageJ pour mesurer la taille et la morphologie, et par EDS (Spectroscopie dispersive en énergie des rayon X) pour la composition chimique. Les résultats montrent que l'atmosphère de synthèse influence beaucoup la taille et l 'uniformité des particules. L'hydrogène donne des particules plus pures mais plus grosses et moins régulières pour l'argent, alors que l'argon favorise la nucléation et produit des particules plus petites et homogène. Pour le cuivre, les température intermédiaires (600 - 650°C) donnent des particules petites, pures et uniformes adaptés aux applications électroniques, tandis que 700 °C produit des particules encore plus petites mais agglomérées, utiles pour la catalyse. Pour les poudres Cu-Ag, le rapport précurseur influence la stabilité et la résistance à l'oxydation : le rapport 1 :1 donne des particules petites et uniformes avec une structure cœur-coquille sans oxydation, tandis que le rapport 1 :3 provoque un regroupement et une oxydation après stockage. Ce travail confirme que l'atmosphère gazeuse, la température et le rapport précurseur sont essentiels pour ajuster les propriétés des nanoparticules et propose de nouvelles pistes pour concevoir des poudres bimétalliques avec des surfaces et une stabilité contrôlée.

Mots-clés : Pyrolyse par pulvérisation ultrasonique ; Réduction de l'hydrogène ; Nanoparticules ; Poudres bimétalliques ; Atmosphère gazeuse ; Rapport précurseur ; Température de réduction.

Table of contents

List of figures

List of tables

Acronyms and Abbreviations

AFM : Atomic Force Microscopy

Ag : Chemical symbol for silver

AgNPs : Silver nanoparticles

Ar : Argon

Cu : Chemical symbol for copper

MEB : Microscopie électronique à balayage

CuNPs : Copper nanoparticles.

DLS : Dynamic Light Scattering

EDS/EDX : Energy-dispersive X-ray Spectroscopy

FTIR : Fourier-transform Infrared Spectroscopy

HR : Hydrogen reduction

H_2 : Hydrogen gas

NPs : Nanoparticles

SEM : Scanning Electron Microscopy

SIMS : Secondary Iron Mass Spectrometry

TEM : Transmission Electron Microscopy

USP : Ultrasonic Spray Pyrolysis

XRD : X-ray Diffraction

Wt% : Weight percent–expresses elemental composition

GENERAL INTRODUCTION

GENERAL INTRODUCTION

Metals have played a significant role in human development throughout history. The early discovery and use of materials like copper and silver helped shape how people lived, created, and organized their societies. These metals enabled the construction of essential tools, weapons, and systems that supported economic growth and social change. Today, they remain deeply embedded in our modern world, supporting nearly every aspect of innovation, from energy and transport to electronics and healthcare. Among the most critical metals in this transformation are copper (Cu) and silver (Ag). Their high conductivity and resistance to corrosion make them indispensable in technologies ranging from electronics and solar energy to biomedical devices. Recent research shows that Cu-Ag nanostructures have properties that neither metal has alone, which makes them incredibly useful in fields like catalysis and biomedical applications (Mallikarjuna & Kim, 2018; Xiong, 2017). In addition to their industrial uses, copper and silver are important from a strategic and economic standpoint. Their applications in defense systems, energy grids, and high-frequency communication make them essential materials in an increasingly digital and electrified world. This dual importance technological and strategic, makes the study of Cu-Ag particularly valuable for future-oriented research.

Fortunately, both copper and silver are highly recyclable. Their ability to retain intrinsic properties after multiple recycling cycles aligns well with circular economy principles. For example, copper can undergo multiple recycling cycles while maintaining its electrical and thermal performance. Currently recycled copper accounts for approximately one -third of global copper demand, demonstrating its significant contribution in offsetting primary extraction and enhancing sustainability in material sourcing (International Copper Association; World Resources Institute, 2024). Likewise, silver is frequently recovered from end-of-life products including electronics, batteries, and medical equipment. As mid of August 2025, silver trades at around US $38 per troy ounce, equivalent to approximately US $1,220 per kilogram (or US $1.22 million per metric ton) (JM Bullion, 2025; Commodity.com, 2025), making its recovery notably more valuable than copper on a per-ton basis (BHP, 2024). This notable price difference has sparked interest in creating copper-silver alloy or composite constructions, which seek to economically integrate the beneficial qualities of both metals (Hong et al., 2023).

Despite these advantages, synthesizing copper-silver (Cu-Ag) powders in a scalable and efficient way remains challenging. A promising approach is Ultrasonic Spray Pyrolysis (USP), where a precursor solution is atomized into fine droplets using ultrasound, then thermally treated to form solid particles. When hydrogen gas is introduced during the process, it enhances the reduction of metal ions and minimizes the formation of unwanted oxides, resulting in purer metallic powders. There is growing interest in nanomaterials in electronics, catalysis, and energy systems which requires synthesis methods that are both efficient and scalable producing high-purity metal powders with controlled morphology. Although USP has focused on its use for Cu-Ag composite with hydrogen-assisted reduction. Furthermore, the effects of synthesis temperature and reduction atmosphere on powder properties remain poorly understood. Addressing these gaps is essential to optimize synthesis strategies and enable new industrial applications. Therefore, this thesis aims to synthesize and characterize copper (Cu), silver (Ag), and copper-silver (Cu-Ag) powders by USP-HR.

Research questions:

- What is the effect of reduction temperature on the shape, purity, and size of Cu, Ag and Cu-Ag powders made using USP?
- What is the effect of using Hydrogen atmospheres during the reduction process?
- How do precursor ratios affect the distribution of Cu-Ag bimetallic powders?

To address these questions, the study is guided by the following hypotheses:

- Higher reduction temperatures are expected to promote more complete reduction but may also cause increased particle agglomeration or morphological deformation.
- It is expected that using hydrogen as the reducing gas will produce powders that are purer and have smoother surfaces than those made in argon-only atmospheres.

Research objectives:

- To synthesize copper (Cu) and silver (Ag) and Cu-Ag powders in the temperature range of 550 to 700 °C

- To compare particle morphology and purity under hydrogen-assisted and non-hydrogen conditions.
- To evaluate the influence of temperature on the structural and compositional characteristics of these powders.

This research is really important because it helps develop simple and scalable ways to make Cu-Ag powders. By improving USP together with hydrogen reduction, this work solves challenges related to cost, purity, and control of particle shape. The results can be useful for electronics, catalysis, and renewable energy systems. They also support recycling and the circular economy.

This thesis has three chapters. Chapter 1 reviews the literature on copper, silver, and Cu-Ag nanoparticles, focusing on synthesis methods. Chapter 2 explains the experimental setup, materials and characterization techniques. Chapter 3 presents and discusses the results, showing the effects of the synthesis conditions. The work ends with a summary of the main findings, the limitations, and ideas for future work.

CHAPTER 1: LITERATURE REVIEW

CHAPTER 1. LITERATURE REVIEW

Introduction

This chapter looks at what researchers have already done in the field of nanoparticles (type of nanomaterial). The first part gives a general overview of nanomaterials, including the different types based on their size and shape, how they are used in different industries, and the main methods used to make them. The second part focuses on a specific technique called Ultrasonic Spray Pyrolysis (USP). It explains how USP works, how it forms particles, and why it is useful for making nanoparticles, along with its benefits and drawbacks, The third part talks about hydrogen reduction; its mechanism, why it's important in making nanoparticles, and how thermodynamics help explain and control the process. Finally, the last part describes the tools used to study and test the materials, looking at their structure, composition and physical properties. The chapter ends by pointing out what's still missing in current research and what could be explored next.

1.1 Overview of Nanomaterials

Nanomaterials are materials with sizes between 1 and 100 nm. At this tiny scale, they behave differently from bulk materials because of their large surface area and special nanoscale effects. These unique properties make them useful for applications like catalysis, sensors, antimicrobial coatings, and conductive materials (Mondal et al., 2024; Wang et al., 2017).

1.1.1 Classification of Nanomaterials

To better understand their properties and applications, nanomaterials are commonly categorized into different groups. Nanomaterials can be classified based on their dimension (shape and size), compositions, or how they are made. This classification helps researchers choose the right type of nanomaterial for specific applications. In this section, the focus will be on the classification based on dimensional characteristics, with particular attention to Cu-Ag nanoparticles, as they are most relevant to the topic of this study.

- **Zero-dimensional nanomaterials**

All dimensions of zero-dimensional (0D) nanomaterials, such quantum dots and

nanoparticles like, are contained inside the nanoscale. Zero-dimensional nanoparticles are among the most prevalent forms of nanomaterials, characterized by all dimensions being within the nanoscale none exceeding 100 nm. These particles are essentially point-like in structure, appearing as small as a single point (V. Singh et al., 2020). Due to their extremely small size, they exhibit unique electronic, optical, and magnetic properties that are not observed in bulk materials. Such properties make them highly attractive or applications in catalysis, bioimaging, and drug delivery systems. And according to Jeevanandam et al. (2018), the most prevalent types of these particles include hollow spheres, nano lenses, quantum dots (uniform particle arrays), etc.

- **One-dimensional nanomaterials**

They have one dimension that extends beyond the nanoscale, while the remaining dimensions remain within the manometer range. Common examples include nanofibers, nanotubes, and nanorods.(V. Singh et al., 2020). Nanowires and nanotubes are examples of one-dimensional (1D) materials, which have one dimension that is noticeably longer than the others. Owing to this geometry, 1D nanomaterials exhibit distinct physical and chemical properties: their extremely high aspect ratio provides an exceptionally large surface area to volume ratio and induces quantum confinement effects in the two confined dimensions, which together result in enhanced surface reactivity and novel electronic and optical properties (Xia et al., 2003). Furthermore, the elongated structure leads to strongly anisotropic behaviour, imparting remarkable mechanical strength along their length and enabling superior electrical conductivity in the longitudinal direction relative to bulk materials (D. Li et al., 2008).

- **Two-dimension nanomaterials**

Compared to nanoscale (100 nm), these kinds of nanomaterials are two dimensions bigger. Among this class, nanofilms, nanolayers, and nanocoating are the most prevalent examples. The structures of this class of nanomaterials resemble plates.(V. Singh et al., 2020). Two-dimensional (2D) materials, such as graphene and nanosheets, are very thin at the nanoscale and have two extended dimensions. Because of their unique geometry, they often display exceptional electronic, optical, and mechanical properties that make them highly valuable in nanotechnology and energy-related applications.

- **Three-dimension nanomaterials**

Three-dimensional nanomaterials possess overall dimensions greater than 100 nm, yet they are composed of building blocks that remain within the nanoscale. These structures are formed through the assembly of nanosized particles and are typically nonporous in nature. They are widely used across various applications due to their unique properties. Nanoscale building pieces assembled in bigger designs, such nanocomposites or porous materials, make up three-dimensional (3D) nanostructures.

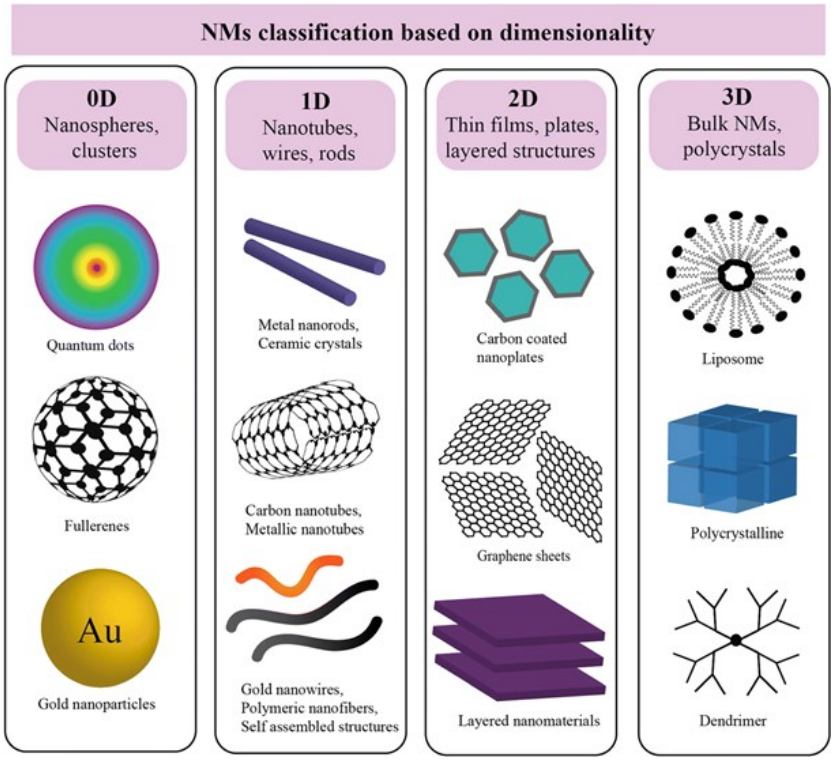

Taken from: (M. A. Darwish et al., 2024)

Figure 1: Classification of nanomaterials on the basis of dimensions

1.1.2 Copper Nanoparticles (CuNPs)

Gawande et al. (2016) explain that copper nanoparticles are studied a lot because copper is cheap and easy to find compared to noble metals. Their small size and large surface area give them unique physical and chemical behaviours, including high electrical and thermal conductivity, catalytic efficiency, and antimicrobial effects (Calderón-Jiménez et al., 2017). These features make CuNPs attractive for applications in biomedical, electronic, and catalytic fields. However, their practical uses is often limited by their tendency to oxidize in ambient conditions, which reduces stability and performance (Tomotoshi & Kawasaki,

2020). Different approaches have been developed to synthesize CuNPs, mainly divided into chemical, biological (green), and physical routes. Chemical methods, such as reduction of copper salts with agents like sodium borohydride or ascorbic acid, are widely used because they allow control over size and morphology (Harishchandra et al., 2020). In recent years, there has been more interest in using green synthesis to make copper nanoparticles, In this method, natural materials like plant extracts, microorganisms, or biopolymers are used as both reducing and stabilizing agents. (Krishna et al., 2024). Some Physical methods, like ball milling and laser ablation, are also used to make CuNPs. However, these techniques usually need special equipment and consume a lot of energy (W. Li et al., 2020). Overall, recent studies emphasize stabilization strategies to improve the air stability of CuNPs, which is critical for their practical use.

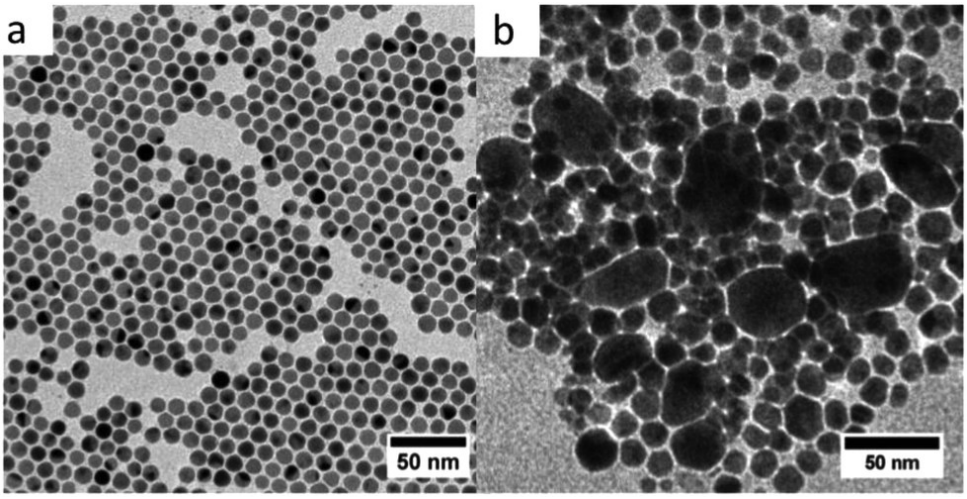

Taken from Ben Aissa et al. (2015)

Figure 2:TEM image of uniform, spherical copper nanoparticles with narrowed size distribution and self-organized spatial arrangement

The morphology of CuNPs synthesized via controlled chemical reduction can be observed in Figure 2 which shows a TEM image of nearly spherical nanoparticles with narrow size distribution. Such structural uniformity is highly desirable for applications in electronics and catalysis, where reproducibe particle size and shape strongly influence performance.

1.1.3 Silver Nanoparticles AgNPs

Silver nanoparticles are notable for strong localized surface plasmon resonance (LSPR) in the visible range and very high electrical/thermal conductivity (Facibeni, 2023). They also

possess intrinsic catalytic activity and broad-spectrum biocidal (antibacterial, antiviral, antifungal) properties. Many AgNPs are spherical (10–30 nm) in transmission electron microscopy (TEM) with average diameter ≈ 20–30 nm, consistent with LSPR absorption peaks around 400 nm.

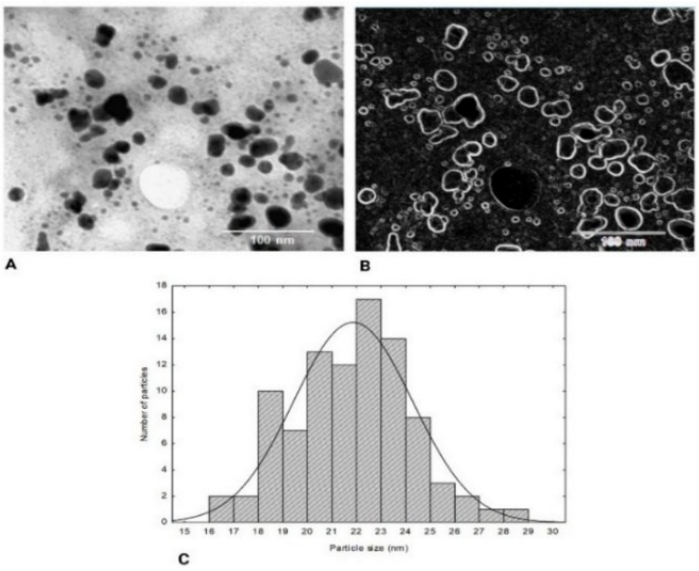

Taken from Pavić et al. (2024)

Figure 3:TEM image and size distribution of spherical silver nanoparticles (AgNPs) synthesized via a fungal extract

The AgNPs in (A) and (B) appear monodisperse and highly crystalline, illustrating the typical morphology of chemically or biologically prepared AgNPs. The size-distribution histogram (C) confirms the mean size, and the high surface-to-volume ratio underlies their enhanced reactivity, plasmonic behaviour, and catalytic efficiency. AgNPs films and nanowires dramatically enhance electrical conductivity in printed electronic, and their tunable LSPR enables ultrasensitive optical sensing. Chemically, AgNPs readily release silver ions under oxidative conditions, which contributes to microbial membranes, generate reactive oxygen species, and disrupt cellular functions. These multimodal biocidal mechanism explain AgNPs' exceptional antibacterial performance (Krishnan et al., 2020).

1.1.4 Copper-Silver Nanoparticles Cu–Ag NPs

Bimetallic nanoparticles are increasingly studied because of they often exhibit superior properties compared to their monometallic counterparts. Among them, Cu–Ag

nanoparticles are notable for their exceptional physical, chemical, and catalytic characteristics (Xiong, 2017). Their enhanced catalytic, thermal, optical, and electrical properties arise from the synergistic interaction between the two metals. Various synthesis routes have been reported, including chemical reduction, seed-mediated processes, galvanic displacement, and thermal decomposition. A particularly common configuration is the Cu core–Ag shell which suppresses copper oxidation and significantly enhances stability during storage and at elevated temperatures. Distinct core–shell architectures have been verified by advanced characterisation techniques such as TEM, XRD, and EDX. Depending on the synthesis procedure, composition particle sizes usually range from 10 to 100 nm. TEM coupled with EDX mapping clearly depicts copper cores encompassed by silver shells, as demonstrated in this figure below.

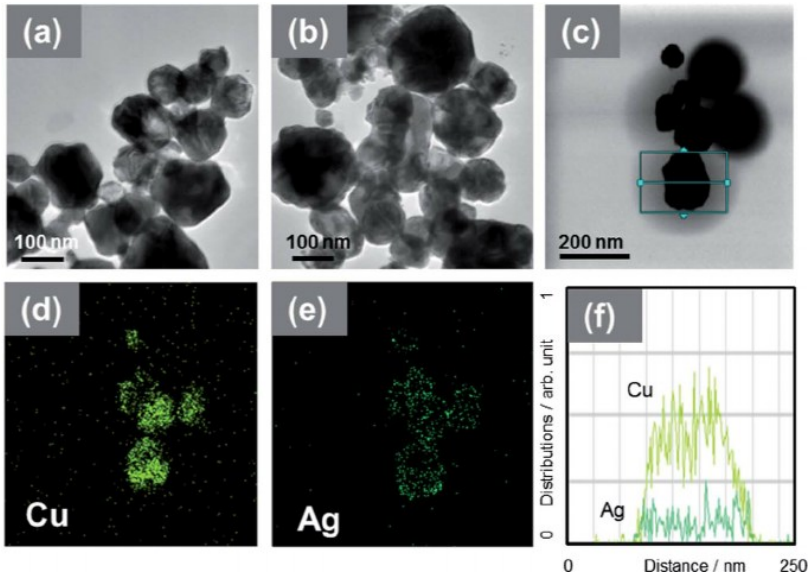

Tahen from Miyakawa et al. (2014)

Figure 4:TEM image and EDS elemental mapping of Cu@Ag core–shell nanoparticles

This architecture not only enhances oxidation resistance but also sustains structural integrity for several months under ambient conditions. In electrochemical CO_2 reduction, increasing the silver content shifts catalytic selectivity toward CO production while suppressing competing hydrogen evolution. Overall, the synergistic interplay between copper and silver in Cu–Ag bimetallic NPs underpins their enhanced performance in catalysis, electronics, and antimicrobial applications context, making them highly promising for next generation technologies (Miyakawa et al., 2014)

1.1.5 Application across sectors of nanomaterials

Due to their exceptional properties, nanomaterials have found applications across a wide range of industries.

1.1.5.1 Catalysis application:

The field of catalysis also benefits from nanomaterials due to their high surface activity and tunable reactivity. To improve the catalyst's efficiency and raise product yields and purities, research into novel catalytic materials or the improvement of current catalyst systems are crucial. Nanoscale catalyst possess high specific surface area and surface energy, which not only enhance their catalytic activity but also improve reaction selectivity by enabling lower reaction temperatures, minimizing side reactions, and allowing for higher recycling efficiency and energy recovery.(Sharma et al., 2015).

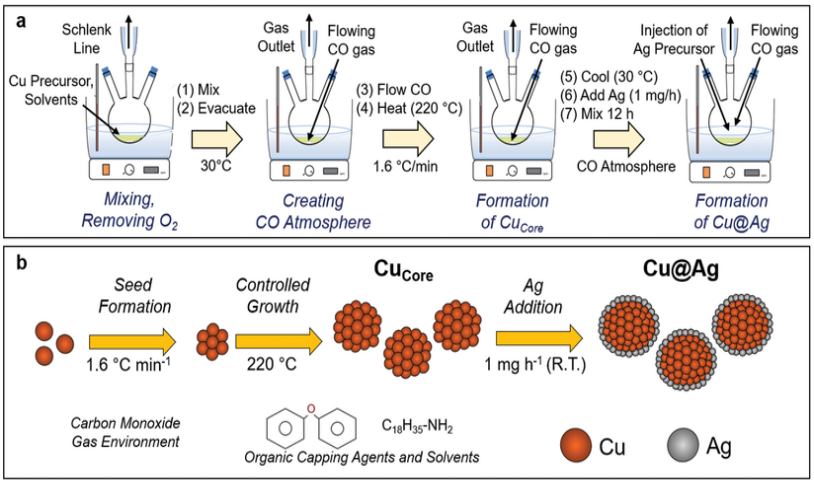

Taken from Kuhn et al. (2021)

Figure 5:Schematic of a Cu@Ag core–shell nanoparticle electrocatalyst

In catalysis, metal nanoparticles such as gold, silver, copper, platinum, and palladium have demonstrated superior catalytic activity compared to their bulk counterparts. For example, silver and silver oxide nanoparticles synthesized via biological routes have shown remarkable catalytic performance in glucose oxidation and other redox reactions, while also exhibiting antimicrobial activity and facilitating electrochemical sensing (Islam et al., 2021). Similarly, metal oxide nanoparticles like ZnO and TiO_2 have been widely used as heterogeneous catalysts, with their activity strongly linked to surface defects and particle size (Wang et al., 2017).

1.1.5.2 Medicine sector

Metal-organic frameworks (MOFs), for instance, provide high porosity and tunable surface chemistry, making them excellent candidates for opto-electrochemical sensors targeting antibiotics and hormones (Oladipo et al., 2023). In addition, silver nanoparticles, especially those synthesized through mycogenic (fungal) methods, have been incorporated into electrochemical glucose sensors, where their high conductivity and electrocatalytic properties enable rapid and sensitive detection (Islam et al., 2021). This application is exemplified in Figure *6* (a), which illustrates an Au@Ag plasmonic glucose sensor operating via oxidative etching of the Ag shell, enabling colorimetric glucose detection.

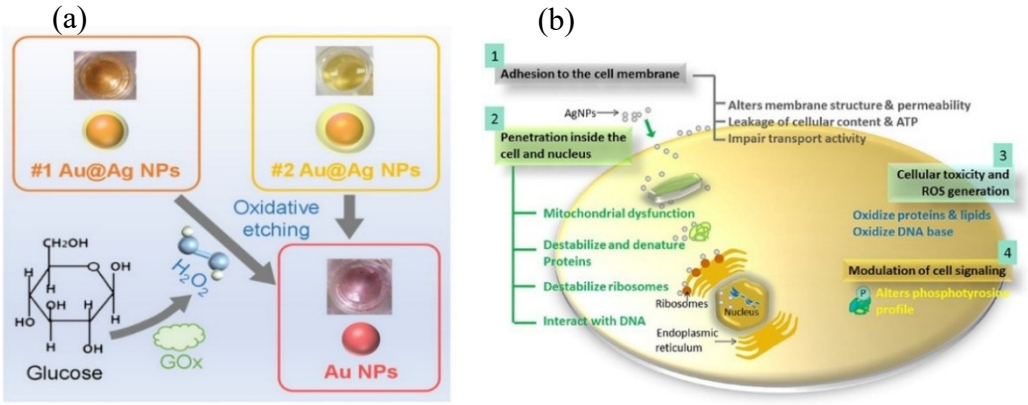

Taken from (Dakal et al., 2016; Nanoparticles, 2022)

Figure 6: Applications of nanoparticles in the medical sector: Sensing (a) and antimicrobial mechanism (b)

Antimicrobial properties are among the most widely studied applications of nanomaterials. Silver nanoparticles are renowned for their broad-spectrum antimicrobial activity, which is attributed to their ability to disrupt microbial membranes, generate reactive oxygen species (ROS), and release Ag^{+} ions that interfere with vital cellular processes (Sahoo et al., 2022; Wang et al., 2017). The antimicrobial efficacy of ZnO and TiO_2 nanoparticles is similarly linked to ROS generation, especially under light activation, making them valuable for disinfection and sterilization (Mondal et al., 2024). Recent studies have also shown that nanomaterials can interfere with bacterial quorum sensing, which is critical for biofilm formation and pathogenicity, thereby enhancing their antimicrobial potential (Hu et al., 2024). Beyond biomedical contexts, copper and silver nanoparticles have also been applied in water treatment, where they are incorporated into membranes, filters, and nanocomposites to achieve disinfection. These systems have demonstrated extremely high

bacterial and viral inactivation rates (often exceeding 99.99%), owing to combined effects of ion release, ROS generation, and biofilm inhibition, making Cu and Ag nanomaterials promising candidates for sustainable water purification. These mechanisms are schematically summarized in Figure *6* (b), which depicts the multiple antimicrobial pathways of silver nanoparticles, including membrane disruption, ROS production, and interference with DNA and proteins (Dakal et al., 2016).

1.1.5.3 Electronics applications:

Among other applications, nanomaterials are utilized in next generation electronics, high energy density batteries and magnetics, durable medical implants, ductile machinable ceramics and premium insulation, satellites and aerospace (Mhetre et al., 2021). Conductive inks based on nanoparticles have garnered a lot of interest recently for flexible and printed electronics. The most popular inks are made using silver nanoparticles because to their superior stability and conductivity. Because they can be printed at low temperatures on plastic or textile substrates, they are used in wearable sensors, RFID antennas, and flexible circuity.

(a) (b)

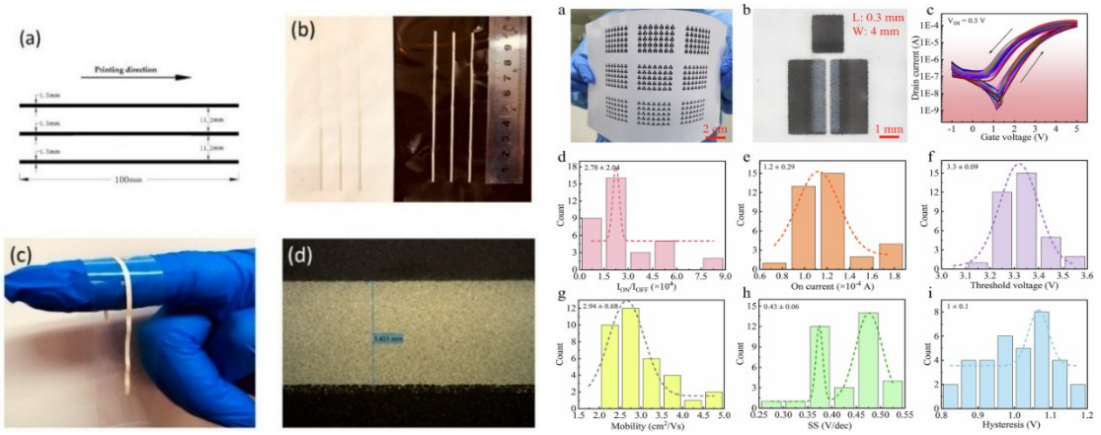

Taken from (X. Li et al., 2025; Zhong et al., 2019)

Figure 7: Applications of nanomaterials in electronics: (a) Conductive inks and (b) Printed transistor performance

Because copper is less expensive than silver, copper nanoparticle inks show promise as well. However, they have the drawback of being easily oxidized, which lowers conductivity. Researchers are creating protective coatings and controlled sintering techniques to address this issue. Figure *7* (a) illustrates the possible application of

stretchable silver conductive ink in wearable electronics by printing an example of the ink on a flexible substrate.

Besides metals, carbon-based and oxide nanomaterials are also used in conductive inks for electronics. Graphene and carbon nanotube inks combine good electrical conductivity with excellent flexibility, which makes them very useful for printed sensors and bendable devices. They are especially promising for chemical and gas sensing applications because of their large surface area and sensitives to adsorbed molecules. Zinc oxide (ZnO) nanoparticles inks are another important example, since ZnO is a wide bandgap semiconductor with applications in transistors, UV detectors, and biosensors. Figure *7* (b) represents a fully printed ZnO transistor array on paper, which shows that nanomaterial inks can be used to fabricate low-cost, large-area, and flexible electronic devices. These advances show how nanomaterials enable the production of lightweight, printable, and highly functional electronics for the future.

1.2 Synthesis methods of nanoparticles:

There are many different ways to create nanoparticles, but they may be generally divided into top-down and bottom-up techniques. The material, desired particle size, purity, and intended use all.

1.2.1 Top-down synthesis technique

Common top-down techniques include mechanical milling, laser ablation, lithography, etching, sputtering, and electro-explosion. Among them, ball milling is one of the most common methods. In this process, large powders are broken down into smaller particles through high-energy impacts. This technique can produce a large amount of nanomaterials, including metals, alloys, and ceramics (Suryanarayana, 2001). However, the particles often end up with irregular shapes, and there is a risk of contamination from the milling equipment. Another important method is laser ablation in liquids (LAL). In this process (figure.8), a strong laser beam is focused on a solid target placed in a liquid. The laser energy breaks the bulk material into very small particles, which then remain suspended in the liquid. This technique is useful because it can produce very pure nanoparticles of metals such as gold, silver and copper without chemical additives, making it suitable for medical, electronic, and catalytic applications (Zhang et al., 2017, Laser Synthesis and Processing

of Colloids: Fundamentals and Applications). Techniques such as lithography, sputtering, and electro-explosion are also widely used, especially in the semiconductor industry, to make thin films and nanoscale structures.

Top-down methods are simple and scalable, but they have some disadvantages. It is often difficult to control the size, shape, and uniformity of the nanoparticles. The methods also require a lot of energy and expensive equipment. As Tripathy (2023) explains, the main drawback of top-down approaches is that they cannot give the same precise control as bottom-up method, which build nanoparticles atom by atom.

1.2.2 Bottom-up synthesis methods:

Bottom-up methods make nanomaterials starting from very small building blocks like atoms or molecules (Baig et al., 2021). Unlike top-down methods, which break big materials into small ones, bottom-up methods build them step by step. These methods often use chemical reactions in liquids, gases, or other controlled ways. Examples include sol-gel, chemical vapor deposition (CVD), microemulsions, and spray pyrolysis methods. In sol-gel and microemulsion methods, the reaction happens in a liquid. CVD makes thin films from gases on hot surfaces. Laser ablation breaks a solid target in a liquid into nanoparticles. In ultrasonic spray pyrolysis (USP), a solution is sprayed and heated to make fine particles. Each method has advantages and limits when controlling particle size, shape, and composition.

1.2.1.1 Sol-Gel method

The sol-gel process is a classic wet-chemical bottom-up route for making nanomaterials. It typically starts from metal alkoxide or salt precursors in solution, which undergo hydrolysis and polycondensation to form a colloidal sol. Over time this sol evolves into a cross-linked gel network containing the desired metal (often oxide) species (Baig et al., 2021). Subsequent drying and heat treatment (calcination) convert the gel into a solid nanostructured material. Because the inorganic precursors are dispersed at the molecular level, sol-gel yields highly homogeneous metal-oxide nanomaterials with the fine control over porosity and composition. Importantly, sol-gel route is relatively simple and low-temperature compared to many other methods: it is economically friendly and produces product that are uniform and easily processed into complex shapes or composites. These

attributes make sol-gel one of the most widely used bottom-up techniques for metal-oxide and composite nanomaterials.

1.2.1.2 Chemical vapor deposition

Chemical vapor deposition is a gas-phase bottom-up method for growing thin films and nanostructures. In CVD, a gas-phase precursor (often an organometallic or hydrocarbon) flows over a hot surface or catalyst and chemically breaks down, leaving a thin film or nanostructured layer on the substate (Baig et al., 2021). For instance, carbon nanotubes are grown by flowing a carbon-rich gas over a metal catalyst at high temperature, causing carbon atoms to deposit and crystallize into tubular nanostructures (Baig et al., 2021). By choosing suitable catalysts and conditions, CVD can yield highly crystalline high-purity materials. It is especially known for producing high-quality two-dimensional materials: for example, monolayer graphene is achieved by CVD on copper catalysts, while nickel or cobalt catalysts give multilayer graphene (Baig et al., 2021). Overall, CVD is regarded as an excellent method for producing high-quality nanomaterials with precise control over structure. Its main limitation is typically that it yields films or coatings on substrates rather than free nanoparticles, but it excels at generating uniform nanoscale layers with excellent crystallinity.

1.2.1.3 Ultrasonic Spray Pyrolysis as a bottom-up Technique

At the core of Ultrasonic Spray Pyrolysis (USP) is a relatively simple but powerful idea: turning a liquid solution into solid powder through sound and heat.

Taken from Stopić et al. (2025)

Figure 8: An advanced setup of the ultrasonic spray pyrolysis (USP) device

In the field of noble metal nanoparticle synthesis, USP is becoming more and more important because it can produce high-quality particles with good uniformity (Majerič & Rudolf, 2020). Compared to other methods, USP is simple, cost-effective, and allows easy control over key parameters like temperature, solution concentration, and gas type (Stopić & Friedrich, 2022). Because of these advantages, USP has been used by many researchers to make silver, copper, and Cu–Ag nanoparticles, which are useful in electronics, sensors, catalysis, and other applications (Stopić et al., 2014).

In this process as shown in (Figure *9*), a liquid solution containing metal salts (called precursors) is broken into tiny droplets using ultrasonic waves.

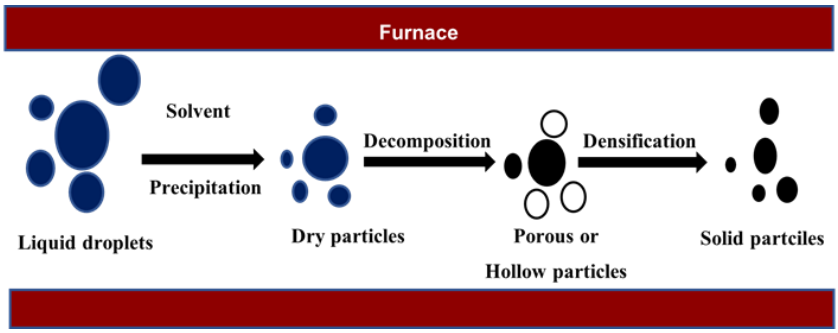

Adapted from Bang and Suslick. (2010)

Figure 9: Simplified USP process

These droplets are carried by a gas into a hot furnace, where the liquid evaporates and the metal salts break down to form solid particles. The resulting nanoparticles are collected at the end of the reactor or in a filter system. An important parameter in this process is the residence time (τ), which determines how long the droplets and particles remain in the heated zone. It can be estimated using the relation:

$$(\text{Eq.1}) : \tau = Q/V$$

where V is the furnace hot-zone volume (m^3) and Q is the volumetric gas flow rate ($m^3.s^{-1}$) (Stopić & Friedrich, 2019). A longer residence time generally allows more complete precursor decomposition and particle growth, whereas shorter residence times may lead to smaller, less agglomerated particles. This technique is highly versatile, as the particle size and composition can be tuned by adjusting the precursor solution, gas flow, and furnace temperature.

According to (Majerič & Rudolf (2020), there are two main ways that particles form in

USP: the droplet-to-particle (DTP) mechanism and the gas-to-particle (GTP) mechanism. In the DTP mechanism; which is the most common and most important for this work, each droplet becomes one particle. First, the solvent in the droplet evaporates. Then the precursors inside react and turn into a solid nanoparticle. This usually makes spherical, dense particles with a uniform shape. (Majerič & Rudolf (2020) note that DTP is very useful for making metallic and bimetallic particles because it gives good control over particle size and shape, especially when hydrogen is used as a reducing gas. On the other hand, in the GTP mechanism, volatile species evaporate and then nucleate in the gas phase, often producing smaller, nanostructured particles (Dusko et al., 2017). The metal vapor or gas-phase species then nucleate in the gas phase to form very small, often porous or aggregated nanoparticles. GTP is more common in flame or plasma-based spray processes and less relevant for the production of dense metal particles via USP (Stopić & Friedrich, 2014). In summary, the DTP mechanism is more aligned with the goals of this research, as it enables the synthesis of high-purity, dense Cu, Ag, and Cu–Ag nanoparticles with well-controlled properties using USP and hydrogen-assisted reduction.

The size, shape, and quality of nanoparticles produced by Ultrasonic Spray Pyrolysis (USP) depend heavily on several main parameters**.** First, droplet size, which determines final particle size is controlled by the ultrasonic frequency and power. According to Lang's equation, the average droplet diameter (d) can be estimated as:

$$d = 0.34\left(\frac{8\pi\gamma}{\rho f^2}\right)^{\frac{1}{3}} \quad \text{(Eq. 2)}$$

where γ is the liquid surface tension ($N \cdot m^{-1}$), ρ is the liquid density ($kg \cdot m^{-3}$), and f is the ultrasonic frequency (Hz). The constant 0.34 is an empirical factor derived from Lang's theory, and π is the mathematical constant.

Both the droplet size and the solution's concentration (Cs) affect the particle size (Dp). If no precursors are lost throughout the process, the link between the concentration, various precursor qualities, and the ultimate particle size may be explained by Equation.

$$D_p = D_{ds}\left(\frac{C_s.M_{met}}{M_p.\rho_{met}}\right)^{\frac{1}{3}} \quad \text{(Eq. 3)}$$

Equations (1) and (2) are adapted from (Kostić et al., 2024), where they were applied to model droplet and particle size formation in ultrasonic spray pyrolysis.

With Equations (1) and (2), droplet and particle size can be determined in theory, as shown in figure 10:

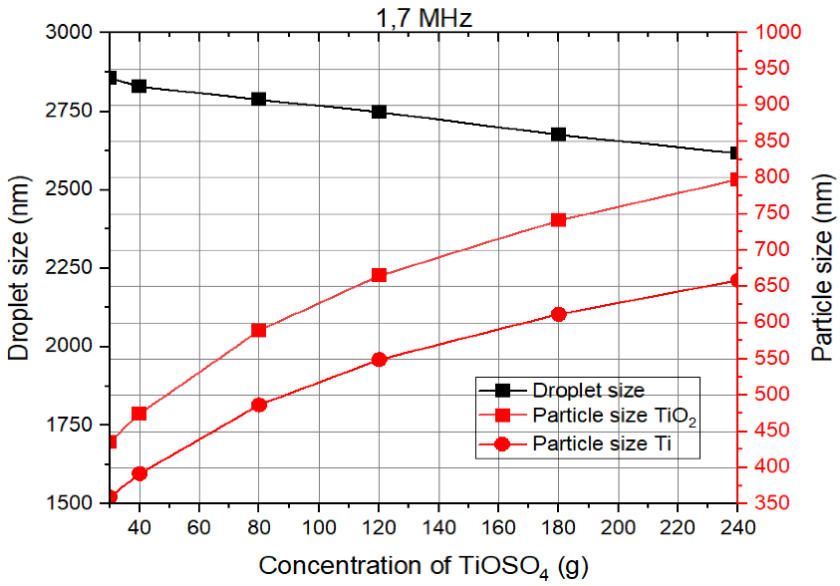

Taken from Kostić et al. 2024)

Figure 10: Droplet and particle size of the titanium powders in theory.

Higher frequencies create smaller droplets, resulting in finer particles (Majerič & Rudolf, 2020). Research shows that adjusting ultrasonic power can reduce average nanoparticle size for instance, silver particles dropped from ~176 nm to ~100 nm by increasing ultrasonic power. Second, the concentration of the precursor solution affects particle size and morphology: lower concentration typically leads to smaller particles.

A number of benefits make Ultrasonic Spray Pyrolysis (USP) a potential technique for creating nanomaterials. Its capacity to provide scalable and continuous manufacturing is one of its main advantages, which makes it appropriate for both industrial and laboratory applications(Rahemi Ardekani et al., 2019). Each droplet functions as a microreactor, creating uniformly shaped particles even in metals and composites, and the procedure is very easy and doesn't require sophisticated equipment. A variety of applications can be supported by USP's ability to create oxides, noble metals (such Au and Ag), and bimetallic structures (like Ag–Cu and Ag/TiO_2) (Majerič & Rudolf, 2020). Compared to other synthesis methods (table1), USP has the advantage of not needing surfactants or stabilizing agents. So, the atmosphere used in USP is very important. Using hydrogen helps make purer particles and gives better control over their properties. This is why studying hydrogen's role in making nanomaterials is important.

1.3 Use of Hydrogen as a reducing agent

In response to global warming, governments are placing greater emphasis on advancing and adopting low-carbon or carbon-free energy sources. Among these, hydrogen energy stands out as one of the most promising clean energy carriers of the 21st century, thanks to its diverse sources, high efficiency, and minimal carbon footprint. As early as 1999, several countries began incorporating hydrogen-based iron ore reduction into their national energy strategies (Tang et al., 2020)

Hydrogen plays a crucial role in metal heat treatment by creating a reducing environment that inhibits oxidation and contamination, thereby improving the surface quality of materials. Additionally, during metal annealing processes, hydrogen can enhance key mechanical properties such as strength, ductility, and formability. Furthermore, Hydrogen-based steelmaking utilizes hydrogen (H_2) as the reducing agent in ironmaking. In this process, hydrogen is typically produced via water electrolysis, and the only by-product is water vapor (Tang et al., 2020).

1.3.1 Mechanism and principle of H_2 in nanoparticle synthesis

For the development of new materials, controlling the production of nanoparticles is crucial. Chemical reduction is often employed, and the result is greatly influenced by the reducing agent selection. One notable substitute for conventional chemical reductants that is both safe and efficient is hydrogen gas.

The process or mechanism of hydrogen reduction is the direct interaction of molecular hydrogen with metal precursors, usually at high temperatures, and occasionally in combination with techniques such as ultrasonic spray pyrolysis. The procedure guarantees a high degree of product purity by reducing metal ions to their elemental state, with water frequently being the only waste.(Hanapin, 2023; Lu & An, 2015; Stopic et al., 2024) General reaction:

$$\text{Metal salt} + H_2 \longrightarrow \text{Metal nanoparticle} + \text{By-product } (H_2O)$$

Compared to other reducing agent (*Table 1*), Hydrogen is a cleaner and greener option for nanoparticles as well need careful handing because it can be dangerous.

Table 1:Comparison between Hydrogen and other reducing agents in NPs synthesis

Reducing agent	Speed & Efficiency	Purity of product	Environmental impact	Control over shape/Size
Hydrogen (Hanapin, 2023 ; Velgosova et al., 2022)	-Moderate to high -Slower than $NaBH_4$ in many cases	-Produces very pure metals -By-product is only water	-Green/reduces environmental risk	-Limited fine tuning of particle size and shape -Does not act as a stabilizer or surfactant
Sodium borohydride ($NaBH_4$) (Velgosova et al., 2022)	-Very fast reduction -Almost immediate reaction	-Can leave chemical residues/stabilizers in products	-May generate hazardous by-products	-Fast nucleation -But may cause aggregation or polydispersity (Journal of Membrane Science, 2020)
Trisodium citrate (TSC), PVP (Velgosova et al., 2022)	-Slower than $NaBH_4$ -Requires more time or complete reduction	-May act as capping agents improving stability	-Generally benign, but may still require washing	-Can tune shape and size -Useful in anistropic/complex morphologies
Ascorbic acid (Vitamin C)	-Moderate	-Low toxicity, but sometimes less pure product	-Green, safe	-Slower nucleation favors larger or more uniform particles (Larm et al., 2025)

1.3.2 Thermodynamic analysis of the hydrogen reduction process

The hydrogen reduction step is critical part of the entire synthesis process (USP). It determines whether the resulting powders will have the right structure, purity and performance for their intended use. Understanding the thermochemistry behind hydrogen reduction is essential. Thermodynamic tools such as Pourbaix diagrams, Gibb's energy (ΔG), and standard redox potentials are often used to analyze how copper, silver etc… behave in a hydrogen rich environment (Rukini et al., 2022). Thermodynamic analysis helps scientists plan and improve the synthesis process. It can predict if a reaction will happen, what products will form, and how different conditions can change the results. In the case of Cu-Ag nanoparticles made from copper and silver nitrates, controlling the hydrogen reduction process is very important. By looking at how Gibbs free energy and reaction balance change with temperature, hydrogen pressure, and the starting materials, researchers can develop better ways to make high-quality, well-controlled bimetallic nanoparticles for advanced applications.

The following equations (4) and (5) predict the predicted reaction of the thermal decomposition of copper and silver nitrate.

$$2AgNO_3 = 2Ag + 2NO_2(g) + O_2\,(g) \qquad \text{(Eq. 4)}$$

$$2Cu(NO_3)_2 = 2CuO + 4NO_2(g) + O_2(g) \qquad \text{(Eq. 5)}$$

The key reduction reactions in the hydrogen atmosphere are:

$$AgNO_3 + H_2 \rightarrow Ag + NO_2(g) + H_2O \qquad \text{(Eq. 6)}$$

$$Cu(NO_3)_2 + 2H_2(g) \rightarrow Cu + 2NO_2(g) + 2H_2O \qquad \text{(Eq. 7)}$$

These thermal decomposition and reduction reactions have been reported in previous studies on nitrate reduction and hydrogen-assisted synthesis of metal powders (Köroğlu et al., 2021).At higher temperatures, these reactions are thermodynamically advantageous; the standard Gibbs free energy becomes more negative, suggesting more spontaneity for the reduction steps.

Research on the one-step hydrogen reduction of combined $Cu(NO_3)_2$ and $AgNO_3$ showed that both metals may be reduced and a controlled bimetallic nanoparticle product can be generated when the right thermodynamic conditions are satisfied (enough temperature and

hydrogen supply) (Köroğlu et al., 2021).

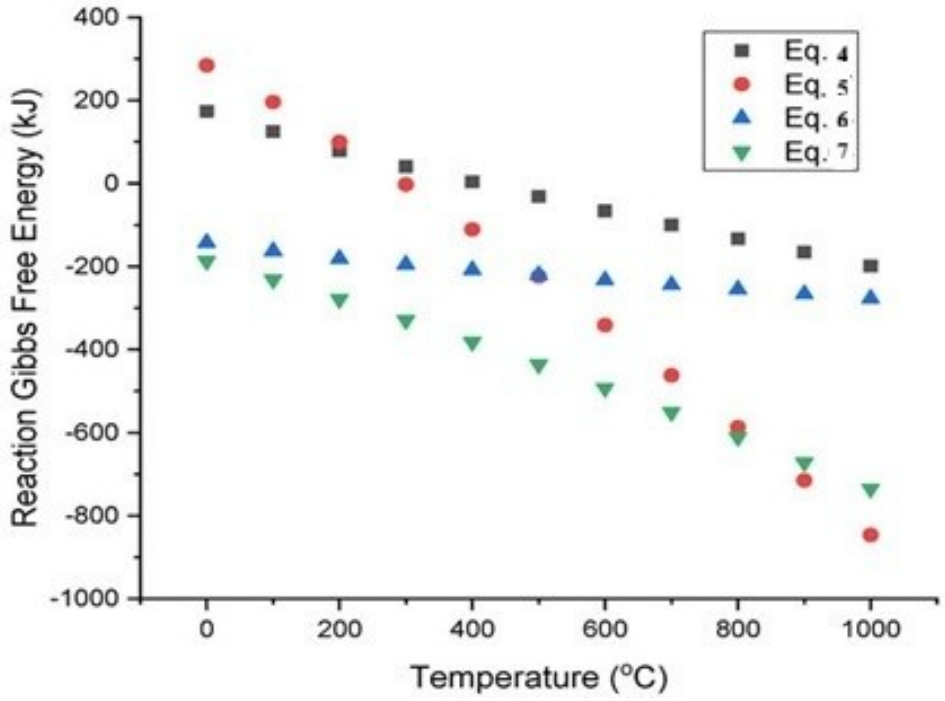

Figure 11: Gibbs free energy change for the HR of silver and copper nitrates

Adapted from (Köroğlu et al., 2021)

Even at ambient temperature, negative Gibbs free energy values show that the hydrogen reduction of $AgNO_3$ and $Cu(NO_3)_2$ is thermodynamically advantageous. However, in a nitrogen environment, their thermal breakdown necessitates higher temperatures, starting at around 420°C for $AgNO_3$ and 390°C for $Cu(NO_3)_2$, at which point the Gibbs free energy turns negative. These results validate the possibility of producing copper and silver by hydrogen reduction of their respective nitrates.

1.4 Nanoparticle characterization:

Nanoparticle characterisation is the process of analyzing the properties, composition, and behavior of materials at the nanoscale. It provides essential information on composition, size, shape, surface properties, crystal structure, and other pertinent aspects, helping researchers understand how nanomaterials differ from their bulk counterparts (A. Singh et al., 2024). Since nanomaterials often exhibits unique behavior that only appear at such small dimensions, accurate characterization is crucial for unlocking their scientific and

industrial potential. The specific analysis methods used in this study are described in the table below.

Table 2:Tools for characterizing materials to examine their characteristics

Types	Characterizations	Objectives
Imaging techniques	Scanning Electron Microscopy (SEM)	provides morphological analysis and surface imaging for nanomaterials.
	Transmission Electron Microscopy (TEM)	High-resolution photos that display atomic-level details can show the internal structure of nanomaterials.
	Atomic Force Microscopy (AFM)	produces surface topography pictures and does nanoscale force measurements.
Spectroscopic techniques	X-Ray Diffraction (XRD)	establishes the phase composition and crystal structure of nanomaterials.
	Fourier-Transform Infrared Spectroscopy (FTIR)	finds the functional groups and chemical bonds in nanomaterials.
	Raman spectroscopy	provide details on the composition and vibrations of molecules.
Surface Analysis techniques	X-Ray Photoelectron Spectroscopy (XPS)	investigates the chemical composition and oxidation states on the surfaces of nanomaterials.
	Secondary Ion Mass Spectrometry (SIMS)	gives information about surface elements and isotopes.
Dynamique measurement techniques	Dynamic Light Scattering (DSL)	determines how the nanoparticles in a liquid medium vary in size.
	Zeta Potential Measurement	evaluates the stability and surface charge of nanoparticles.
Mechanical Characterization technique	Nanomechanical Testing	establishes the mechanical characteristics of nanomaterials, including their tensile strength, elasticity, and hardness.
Thermal Analysis Technique	Nanoscale Thermal Analysis	evaluates the thermal characteristics of nanomaterials, such as their heat capacity and thermal conductivity.

Adapted from (A. Singh et al., 2024)

According to Köroğlu et al (2021), while monometallic Cu and Ag powders have been widely studied, systematic research on Cu-Ag bimetallic system remains markedly underexplored in the literature. Notably, as mentioned earlier there are few investigations examining how different synthesis conditions, for example, using a hydrogen reducing atmosphere versus an inert argon atmosphere, or varying the Cu:Ag precursor ratio affect the structure and properties of Cu-Ag powders. According to Xu et al. (2024), this

underrepresentation can be attributed in part to practical challenges: copper and silver are immiscible at ambient temperature (often yielding phase-segregated microstructures). And base on Köroğlu et al (2021) research, their disparate reduction kinetics and lattice parameters make co-reduction and alloy formation difficult. Another reason or this research gap is practical and historical: Cu-Ag alloys have not been as commercially attractive as other noble- metal alloys, perhaps due to limited imidiate commercial applications and the dominance of monometallic studies. As a result, many questions remain open like how initil metal rati influence particle size and phase behavior (alloy or core-shell or segregated phases) can improve the oxidation resistance of Cu-based nanoparticles. These gaps in understanding clearly undercore the motivation for the present study.

Partial Conclusion

In summary, Cu, Ag, and Cu–Ag nanoparticles show unique physicochemical properties with wide applications, and USP–HR offers a promising synthesis route due to its scalability and ability to enhance purity.

CHAPTER 2: METHODOLOGY

CHAPTER 2. METHODOLOGY

Introduction

This chapter describes the experimental methods used to accomplish the goal of the study, which was to synthesize and characterize powders of copper, silver, and Cu–Ag. It begins with a description of the materials and chemical precursor solutions used in the experiments followed by an overview of the Ultrasonic Spray Pyrolysis (USP) setup and the synthesis parameters. A detailed description of the subsequent Hydrogen-Assisted Reduction (HR) procedure follows. Finally, the chapter outlines the characterisation techniques and software tools used to analyze and interpret the data.

All experimental work was carried out at the IME Process Metallurgy and Metal Recycling Institute RWTH Aachen University (52072 Aachen, North Rhine–Westphalia, Germany), where the synthesis equipment, analytical instruments, and software tools required for the study were available. The institute is internationally recognized for its expertise in metallurgical process development and sustainable metal recycling. Its location within the city of Aachen, a leading hub for science and engineering research in Germany, provided an excellent environment for conducting the present work.

Taken from Google

Figure 12: Font view of the IME Process Metallurgy and Metal Recycling Institute

2.1 Materials

The main precursors used were copper nitrate trihydrate ($Cu(NO_3)_2.3H_2O,$) and silver nitrate ($AgNO_3$), both from Merck KGaA (Darmstadt, Germany) with 99,9% purity taken from the institute's stock. Deionized water was used to dissolve the salts and prepare the precursor solution.

(a) (b)

Figure 13: copper nitrate (a) trihydrate and silver nitrate (b)

These substances were chosen due to their high-water solubility and frequent usage in spray-based synthesis techniques. They are ideal for laboratory-scale ultrasonic spray pyrolysis investigations due to their clean thermal breakdown and high availability. Because it offers a neutral and impurity free medium, deionized water was selected as the solvent to assist guarantee uniformity and dependability in the synthesis process.

2.2 Instrumentation

During preparation and sample processing, a few common laboratory instruments were employed.

Figure 14: Equipment's employed for weighing, solution preparation, and sample storage

For the precursor solutions, the copper nitrate trihydrate and silver nitrate were carefully weighed using an analytical balance. To precisely transport the prepared solutions into the

synthesis system, graduated cylinders were utilized, and beakers were used to estimate and mix the necessary solution quantities. After being gathered, the powders were kept in centrifuge tubes, which facilitated the labelling handing and arrangement of the samples before to analysis.

2.3 Precursor preparation

2.3.1 For the formation of copper (Cu)

To prepare the precursor solution for copper nanoparticle synthesis, 120.8 g of copper nitrate trihydrate ($Cu(NO_3)_2.3H_2O$) was accurately weighed, based on mass formula, to obtain a final concentration of 1 mol/L in 500 mL according to the institute's SOP (Standard Operating Procedure). The powder was gradually added to deionized water and stirred gently with a magnetic stirrer to promote complete dissolution. After a short time, a clear and homogeneous blue solution was obtained, indicating the salt had fully dissolved.

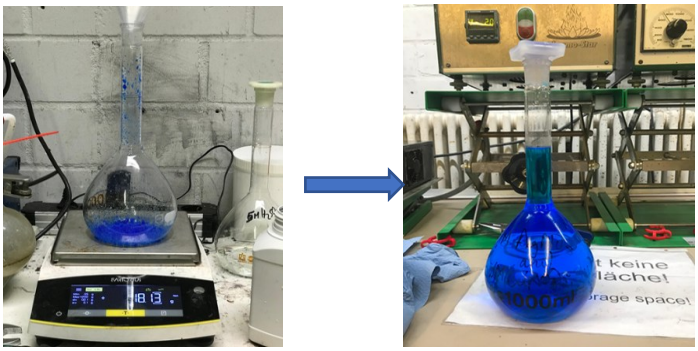

Figure 15: Preparation of copper precursor solution S1(1 M)

Table 3:Parameters used to prepare copper nitrate trihydrate solution

Chemical	Molar mass (g/mol)	Volume (L)	Concentration (L/mol)	Mass required (g)
$\boldsymbol{Cu(NO_3)_2.3H_2O}$	241.6	0.5	1	120.8

2.3.2 For the formation of silver (Ag)

Following the same procedure as described for copper precursor, a 1 mol/L silver nitrate ($AgNO_3$) solution was prepared by dissolving 84.94 g of $AgNO_3$ in 500 mL of deionized water. The resulting solution was clear and homogeneous, indicating complete dissolution

of the silver nitrate. This stock solution was subsequently used for further dilutions and preparation of Ag-containing precursor mixtures. Care was taken to protect the solution from light exposure to prevent photodecomposition of Ag^+ ions.

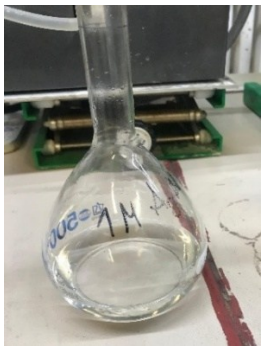

Figure 16: Precursor solution of silver nitrate **S2** (1 M)

Table 4: Parameters used to prepare silver nitrate solution

Chemical	**Molar mass (g/mol)**	**Volume (L)**	**Concentration (L/mol)**	**Mass required (g)**
$AgNO_3$	169.87	0.5	1	84.94

2.3.3 For the formation of copper–silver (Cu-Ag) alloys

Two Cu–Ag bimetallic precursor solutions were prepared from the same materials at different molar ratios.

(a) (b)

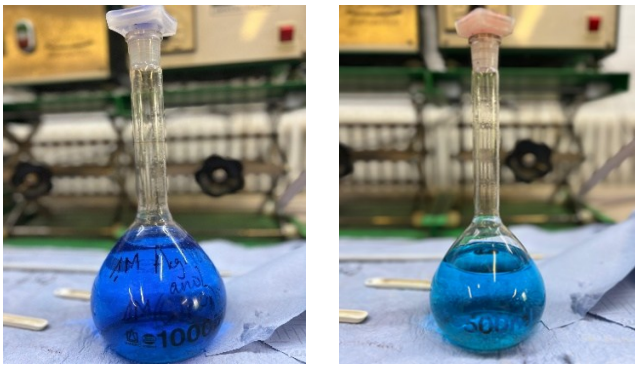

Figure 17 : Cu–Ag precursor solutions: (a) **S3** and (b) **S4**

In the first preparation, equal molar concentrations (0.5 mol/L each) were targeted. Based on molar masses of 241.6 g/mol for $Cu(NO_3)_2.3H_2O$ and 169.87 g/mol for $AgNO_3$, 60.40

g and 42.47 g of each salt were weighed, respectively, and dissolved in 500 ml of deionized water to obtain a homogeneous mixed solution (**S3**). In the second preparation, a (1:3) Cu:Ag molar ratio was used, corresponding to 0.25 mol/L copper nitrate trihydrate and 0.75 mol/L silver nitrate in a final volume of 1 L. For this 127.40 g of $AgNO_3$ and 60.40 g of $Cu(NO_3)_2.3H_2O$ were accurately measured and dissolved under the same conditions (**S4**). The use of two different Cu:Ag ratios allows to compare the effect of different Cu:Ag precursor ratios (1:1 and 1:3) on the properties of the resulting bimetallic powders, in order to assess how compositional variation influences their structural, catalytic, and oxidation-resistance characteristics.

Table 5: Parameters used to prepare solutions S3 and S4

Chemical	Molar mass (g/mol)	Volume (L)	Molar Ratio	Mass required (g)
Cu $(NO_3)_2 \cdot 3H_2O$ and AgNO3 (**S3**)	241.6 and 169.87	0.5	1:1	60.40 for Cu and 42.47 for Ag
Cu $(NO_3)_2 \cdot 3H_2O$ and AgNO3 (**S4**)	241.6 and 169.87	1	1:3	60.40 for Cu and 127.40 for Ag

In the next step, Ultrasonic Spray Pyrolysis combined with Hydrogen Reduction was employed to convert these liquid precursors into Cu, Ag, and Cu–Ag powders with controlled properties.

2.4 Method: (USP–HR)

In this study, copper (Cu), silver (Ag), and copper-silver (Cu-Ag) powders were made using Ultrasonic Spray Pyrolysis (USP) combined with Hydrogen reduction (HR). this method works by turning a liquid solution into tiny droplets, which are then heated. During heating, the droplets turn into solid particles and hydrogen helps to reduce the metal salts. This process makes fine and uniform powders in a continuous way. The process began by setting the desired temperature on the furnace. Once heating was initiated, the precursor solution was poured into a funnel connected to an ultrasonic atomizer. The atomizer operated at a frequency of 1.7 MHz, generating fine aerosol droplets from the solution. These droplets

were then carried into a horizontal tubular quartz reactor by argon gas flowing at 1 L/min.

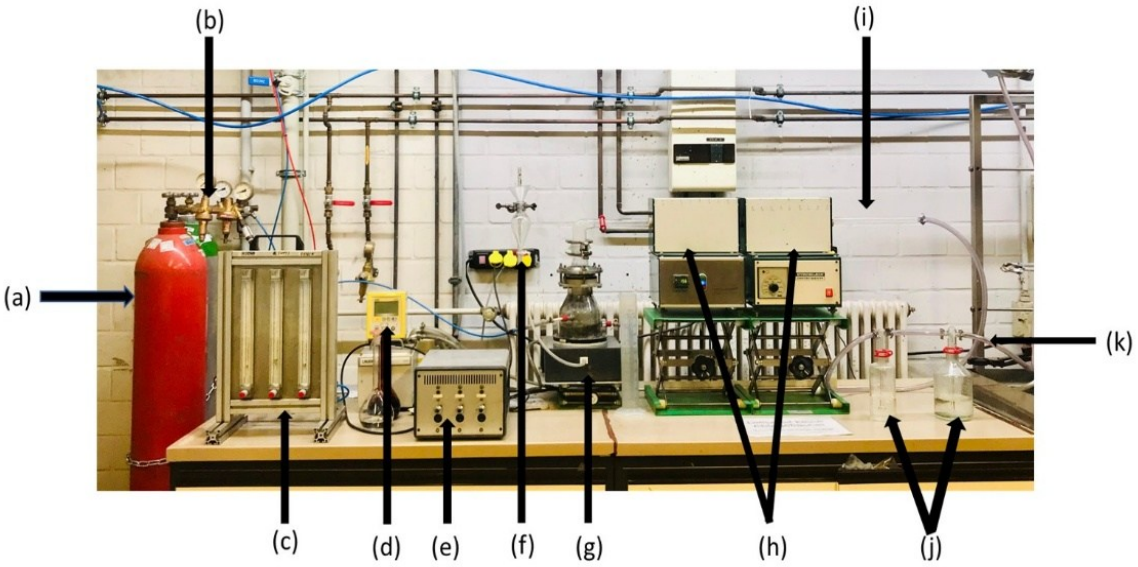

Figure 18: Thermostat setup for USP-HR technique with (a) hydrogen and (b) argon gas bottles, (c) rotameter, (d) thermostat, (e) transformer (f) precursor input, (g) atomizer, (h) furnace, (i) silica tube, (j) wash bottles, (k) exhaust gas.

The quartz tube measured 83 cm in total length with an inner diameter of 2.35 cm. Of this, 61 cm was heated by the furnace, while 11 cm at each end remained unheated. Inside the heated zone, the aerosol droplets underwent: evaporation of the solvent, decomposition of the metal salts, and formation and densification of particles. The calculated residence time using (Eq.1) in the heated zone was approximately 15.8 seconds with argon flow only and 7.9 seconds after the introducing of hydrogen gas, which was supplied at 1 L/min as a reducing agent once the desired temperature had stabilized. This step converted the metal precursors into their metallic forms. For safety reasons, argon was also used at 1 L/min before and after each experiment to purge the system and avoid any hydrogen build-up. To prevent overheating to the ultrasonic transducer, the atomizer temperature was kept constant at 23°C using a water-cooling system controlled by a thermostat. At the end of the reactor, wash bottles were connected to collect the particles, and the exhaust gases were safely vented to the outside atmosphere through a pipe.

2.4.1 Synthesis of Copper (Cu)

The synthesis of copper (Cu) powder was carried out using copper nitrate trihydrate (**S1**)

as the starting material. The process was performed at different temperatures ranging from 550 to 700 °C, to investigate the influence of temperature on the particle properties. The procedure followed was the same as described in the USP–HR method (Figure *18*). As an illustration, one of the Cu synthesis steps conducted at 550 °C using the USP setup is presented in the figure below, showing the preparation and processing stages involved in the experiment.

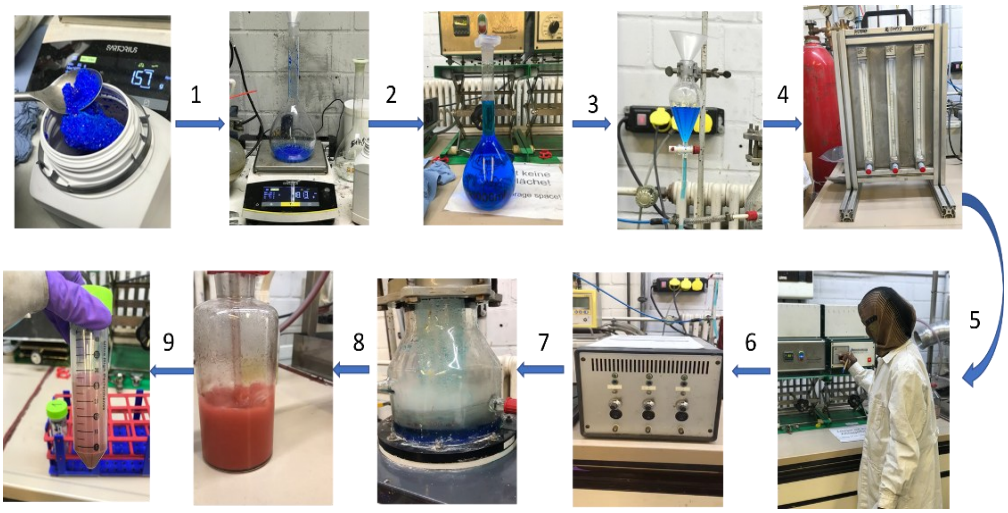

Figure 19: Schematic Representation of Cu Nanoparticle Synthesis steps via USP-HR

Table 6:Experimental conditions used for the synthesis of copper

Solution	Sample code	Temp. °C	Time (min)	H_2/Ar ratio
S1	Cu-1	550	180	1:1
	Cu-2	600		
	Cu-3	650		
	Cu-4	700		

2.4.2 Synthesis of silver (Ag)

The primary aim of this synthesis was to produce silver powders and assess how the gas atmosphere, particularly the presence or absence of hydrogen influences their morphology, composition, and purity. To this end, four samples were prepared from a single precursor solution. Two samples were reduced in a 1 L/min hydrogen/argon mixture at 600 °C and

700 °C for 180 minutes. The other two samples were produced without hydrogen, relying on thermal decomposition under pure argon (1 L/min) at the same temperatures for 60 minutes. The shorter processing time for these argon-only runs was chosen to achieve the target product efficiently, without prioritizing nanoparticle yield. This comparison allows for a direct evaluation of hydrogen's role versus an inert atmosphere.

Table 7:Experimental parameters for the synthesis of silver with and without hydrogen

Solution	Sample code	Temp. °C	Time (min)	H_2/Ar ratio
S2	Ag-6	600	180	1:1
	Ag-7	700	180	1:1
	Ag-8	600	60	Only Ar (1L/min)
	Ag-9	700	60	Only Ar (1L/min)

2.4.3 Synthesis of copper-silver alloys (Cu-Ag)

In this synthesis, two sets of Cu–Ag bimetallic powders were prepared using different molar ratios of copper nitrate trihydrate and silver nitrate. As mentioned earlier, the first set of samples was synthesized using a 1:1 molar ratio (0.5 M each) of Cu and Ag. Subsequently, five additional samples were prepared with a 1:3 molar ratio (0.25 M Cu and 0.75 M Ag).

Table.2.3: *Experimental parameters for synthesis of Cu-Ag*

Solution	Sample code	Temp. (C)°	Time (min)	H_2/Ar ratio
S3	12	550	120	1:1
	13	600		
	14	650		
	15	700		
S4	16	650		

After synthesis, the resulting Cu–Ag powders were collected and subjected to detailed characterization to evaluate their structural, morphological, and compositional properties.

2.5 Particle collection and characterization techniques

After each synthesis experiment (Cu, Ag, Cu-Ag), the nanoparticle suspensions were left to settle by natural sedimentation in beakers. A period of approximately 3 hours was sufficient for complete settling. Once sedimentation occurred, the supernatant was removed using a filter-based collection unit connected to a vacuum pump, allowing for careful recovery of the solid particles.

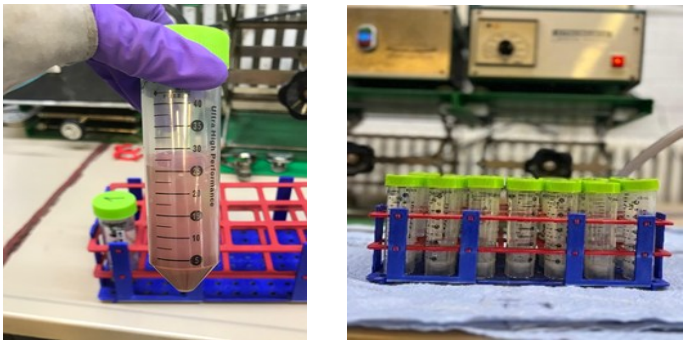

Figure 20: Collected nanopowders in centrifuge tube for analysis

All collected samples were then sent for Scanning Electron Microscopy (SEM) and Energy Dispersive X-ray Spectroscopy (EDS) analysis to examine their morphology and elemental composition. ImageJ software was employed to analyze particle size distribution from the SEM micrographs. After SEM/EDS analysis, the samples were dried and prepared for X-ray Diffraction (XRD) measurements, which were used to determine their crystalline structure and phase composition.

Partial Conclusion

The methodological framework established in this study provided a controlled and reproducible environment for the synthesis of Cu, Ag, and Cu–Ag powders, while allowing systematic variation of critical parameters, although measures were taken to minimize droplet size variation, particle agglomeration, and incomplete reduction, these factors remained practical challenges and potential influences on the final powder characteristics. The next section analyses how the chosen parameters influenced the structure, morphology, and composition of the synthesized powders.

CHAPTER 3: RESULTS AND DISCUSSION

CHAPTER 3: RESULTS AND DISCUSSION

Introduction

This section reports on the properties of copper (Cu), silver (Ag) and bimetallic Cu-Ag nanoparticles produced by ultrasonic spray pyrolysis under hydrogen. We first investigate the effects of gas atmosphere, followed by the influence of synthesis temperature and precursor concentration on elemental distribution, surface characteristics, and particle development. With potential application in catalysis, sensing, antimicrobial etc. in mind, each subsection on Cu, Ag, and Cu–Ag discusses the impact of these factors on nanoparticles size and shape (SEM as well as chemical composition (EDS)

3.1 Silver powders produced via USP and HR

The first objective of this investigation was to examine how the gas environment (H_2 vs. Ar) influences the shape, particle size distribution, and purity of the synthesized nanoparticles. This objective was addressed using silver (Ag) as the model system.

3.1.1 Hydrogen reduction of silver nitrate (AgNPs)

When silver nitrate precursor solution of 1M (**S2**) was introduced into the ultrasonic spray pyrolysis (USP) reactor, it undergoes atomization and droplet formation. In the hydrogen atmosphere at elevated temperatures, hydrogen gas acts as a strong reducing agent, reducing silver ions (Ag^+) to metallic silver (Ag). Thermodynamic calculations predict the overall reactions under USP/H_2 conditions (Köroğlu et al., 2021) as follows:

$$2AgNO_3\,(s) + H_2\,(g) \longrightarrow 2Ag\,(s) + 2HNO_3\,(g) \qquad \text{(Eq. 8)}$$

But at USP temperatures, nitric acid vapors (HNO_3) become unstable and break down further, producing oxygen, water, and nitrogen oxides (NO_x):

$$2AgNO_3\,(s) + H_2\,(g) \longrightarrow 2Ag\,(s) + 2NO_2\,(g) + H_2O\,(g) + \frac{1}{2}O_2 \qquad \text{(Eq. 9)}$$

In this case, hydrogen facilitates the reduction of Ag^+ ions to metallic silver:

$$Ag^+ + e^- \longrightarrow Ag^0 \qquad \text{(Eq 10)}$$

The Gibbs free energy change (ΔG), which is substantially negative for the reduction of Ag^+ to Ag^0 in the presence of hydrogen in the temperature range under study, can be used

to explain the viability of the reduction process as shown in this figure:

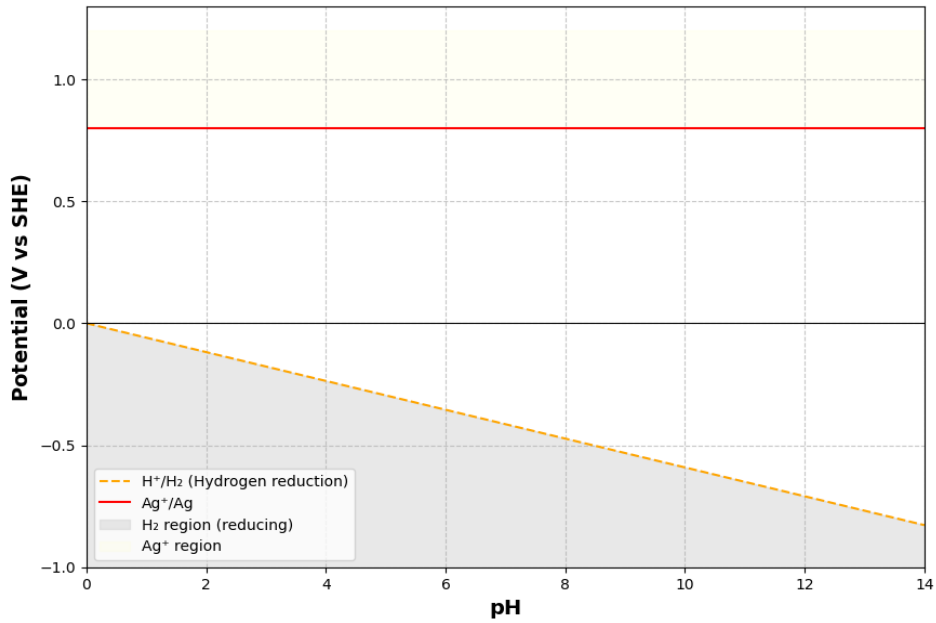

Figure 21: pH–Potential Diagram for Hydrogen Reduction of Silver Nitrate

The orange line in the diagram represents the reduction potential of hydrogen, while the red line indicates the reduction potential of silver. The grey region delineates the conditions where hydrogen's reducing power is enough to convert Ag^+ to metallic to Ag. In contrast, the yellow region highlights the stability of Ag^+ions.

Importantly the diagram demonstrates that hydrogen possesses a sufficiently low reduction potential to reduce $AgNO_3$ directly to elemental silver, without the formation of intermediate oxides. Thus, the thermodynamically stable phase is metallic silver.

3.1.2 Influence of Hydrogen in the morphology and purity of Silver NPs

Building on the reduction mechanism described above, we assessed how the ultrasonic spray pyrolysis with hydrogen reduction (USP–HR) influences particle size. SEM and EDS analyses were performed to evaluate this influence. At 600 °C, SEM micrograph (Figure *22*.a) shows predominantly spherical particles with smooth well-defined surfaces. The particles are fairly uniform in shape and are loosely agglomerated, touching each other but not fused; which suggests limited sintering at this temperature.

Quantitative analysis yields an average particle diameter of 296 nm, with most particles clustering around this size and only a few larger outliers. The relatively modest nucleation

rate allows a smaller number of nuclei to form; those nuclei then grow larger before the available silver is consumed.

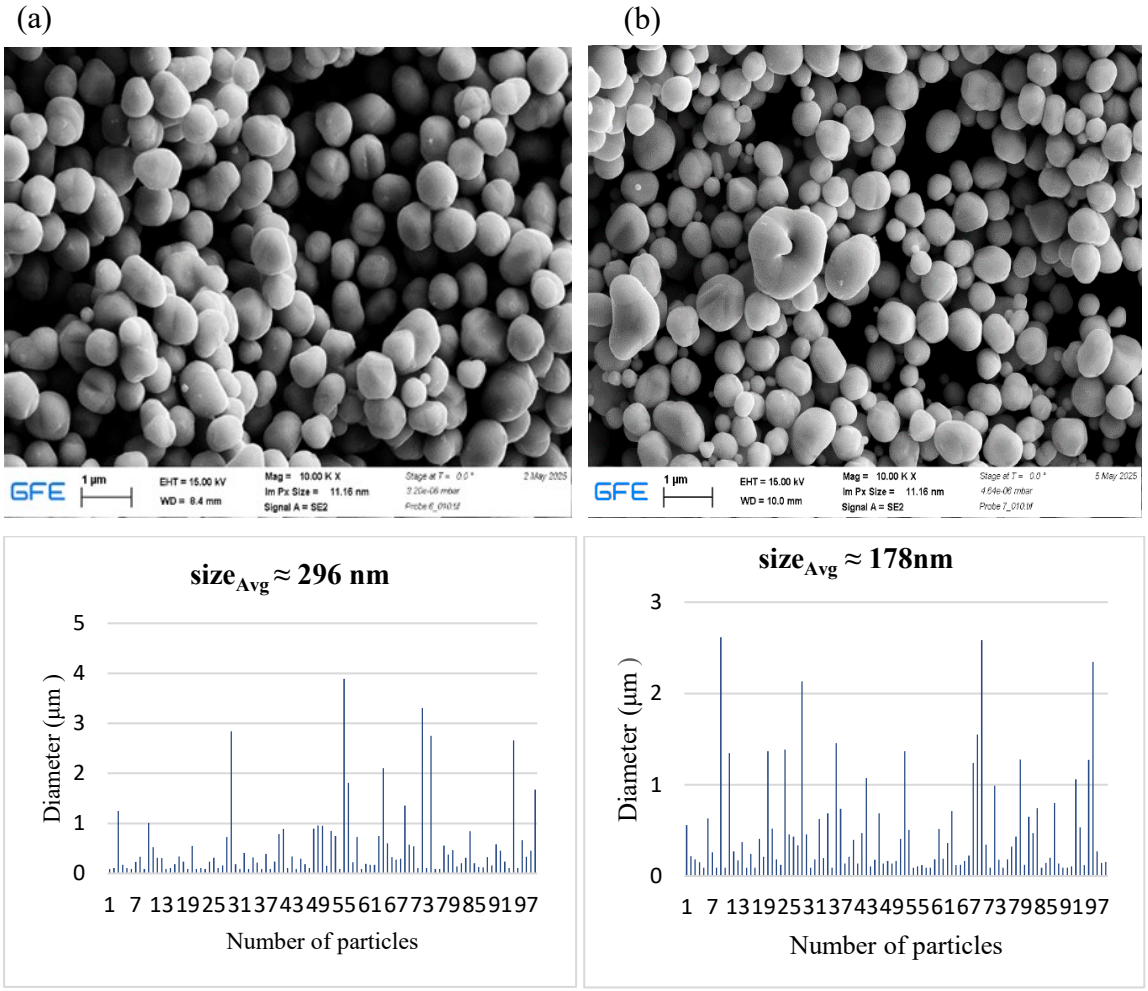

Figure 22: SEM and Particle size distribution of Ag particles (a) 600°C, and (b) 700°C

When temperature was increased to 700 °C, the particles remain spherical and smooth but the distribution is more compact and uniform than at 600 °C. ImageJ analysis shows an average particle diameter of about 178 nm, indicating a significant reduction in size. The higher temperature accelerates solvent evaporation and increases supersaturation in the droplet, triggering a burst of nucleation; many more nuclei form quickly. Because the available silver is divided among more nuclei, each particle remains smaller, yielding a narrower size distribution. Overall, the elevated temperature under hydrogen atmosphere promotes the formation of finer nanoparticles with a more uniform size, while the lower temperature allows fewer nuclei to grow into larger sphere.

Energy-dispersive X-ray spectroscopy of the samples produced at both 600 °C and 700 °C confirms that the particles consist entirely of metallic silver. No other elements or

impurities were detected, indicating that the hydrogen reduction of silver nitrate was complete under all investigated conditions.

(a) (b)

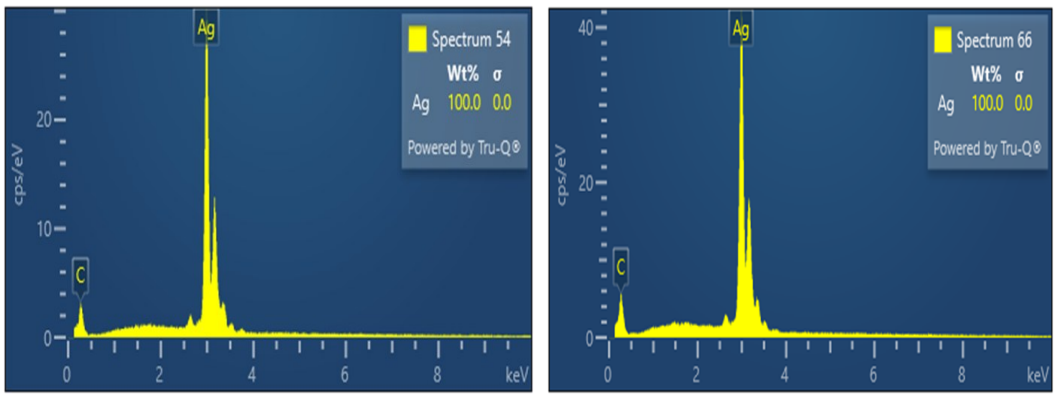

Figure 23: EDS spectrums for Ag particles produced at (a) 600 °C, and (b) 700°C

This high purity underscores again the efficacy of the USP-HR process in converting the precursor to metallic silver without leaving residual nitrate or oxide species. Such purity is critical because the properties of the resulting nanoparticles, including their electrical conductivity and catalytic activity, depend on the absence of contaminants as also highlighted by Krishnan et al. (2020). To compare, silver NPs were also produced without hydrogen, using only argon as the carrier gas.

3.2 Silver powders produced without hydrogen (only Argon)

For this synthesis, the same precursor solution **S2** (silver nitrate) was used, with an argon flow rate fixed at 1 L/min.

(a) (b)

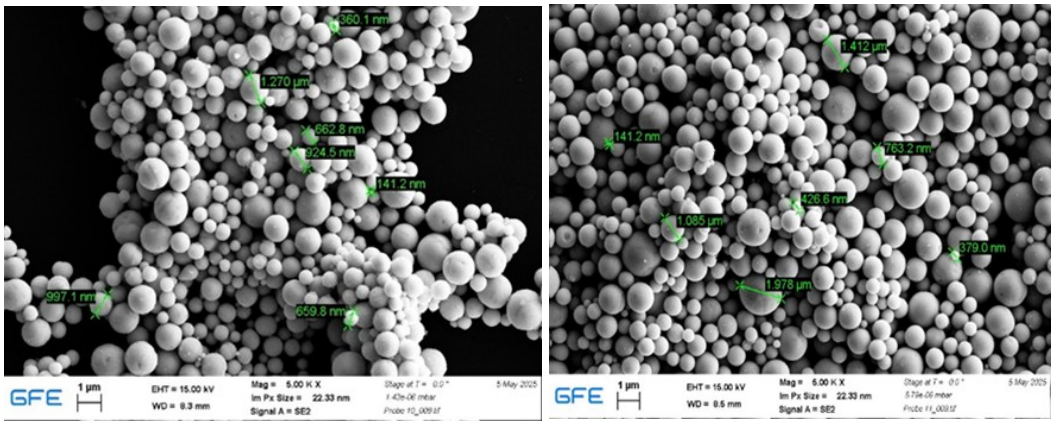

Figure 24: SEM analysis of silver (Ag) (only Ar) at (a) 600 °C, and (b) 700°C

In argon alone, the ultrasonic spray pyrolysis process produced spherical silver particles at

both 600 °C and 700 °C. The SEM micrographs shows that the particles are generally smooth and nearly perfect spheres. At 600 °C the particles population is heterogeneous, with large spheres interspersed among many smaller ones and occasional clusters where particles are noticeably agglomerated. Raising the synthesis temperature to 700 °C yields a more homogeneous arrangement of spheres with improved packing density; the overall distribution appears more uniform, and irregularities in shape are much less pronounced compared to 600 °C sample.

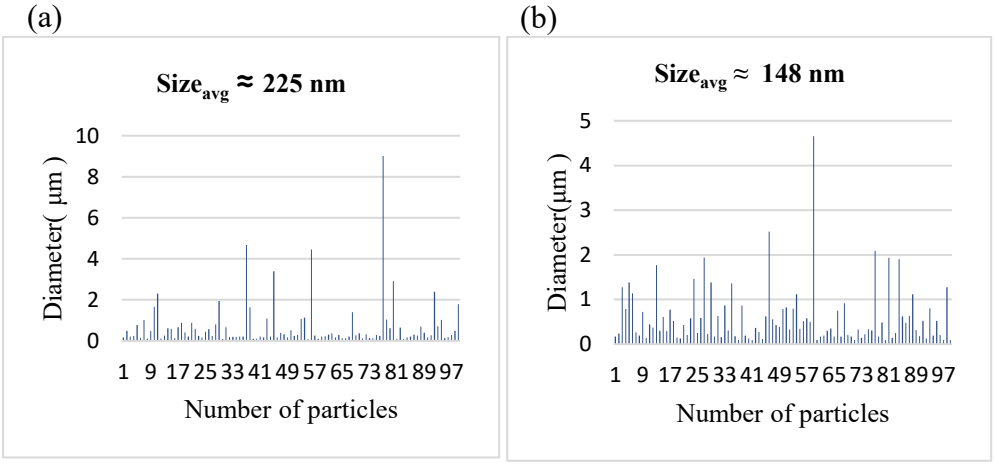

Figure 25: Particle size distribution of silver (Ag) Produced without hydrogen at (a) 600 °C, and (b) 700°C

Quantitative analysis with ImageJ confirms these visual trends. Under argon, the 600 °C sample shows an average equivalent diameter of 225 nm, while the 700 °C sample yields a smaller average diameter of about 148 nm. This decreases in mean size supports the morphological observation that the particle population becomes more uniform and finer at 700 °C. The absence of hydrogen in these syntheses means that the argon atmosphere does not supply any additional reducing species; consequently, particle formation proceeds via thermal decomposition and reduction of the nitrate precursor alone.

Table 8: ImageJ analysis of silver NPs synthesized under argon atmosphere

Condition	Particle count	Average diameter (µm)	Average diameter (nm)	Total projected area (µm²)
600 °C	183	0.225	225	41.204
700 °C	383	0.148	148	56.835

In this inert environment, the lower temperature allows fewer nuclei to form, enabling each particle to grow larger and yielding a broad size distribution. At the higher temperature, the increased solubility and supersaturation of the precursor promote a burst of nucleation, generating many more nuclei; the available silver is divided among them, leading to a population of smaller, more uniformly sized spheres. Thus, while both samples exhibit spherical particles typical of spray-dried droplets, the argon-only atmosphere highlights how temperature controls the balance between nucleation and growth, yielding either coarser or finer particles in the absence of hydrogen reduction.

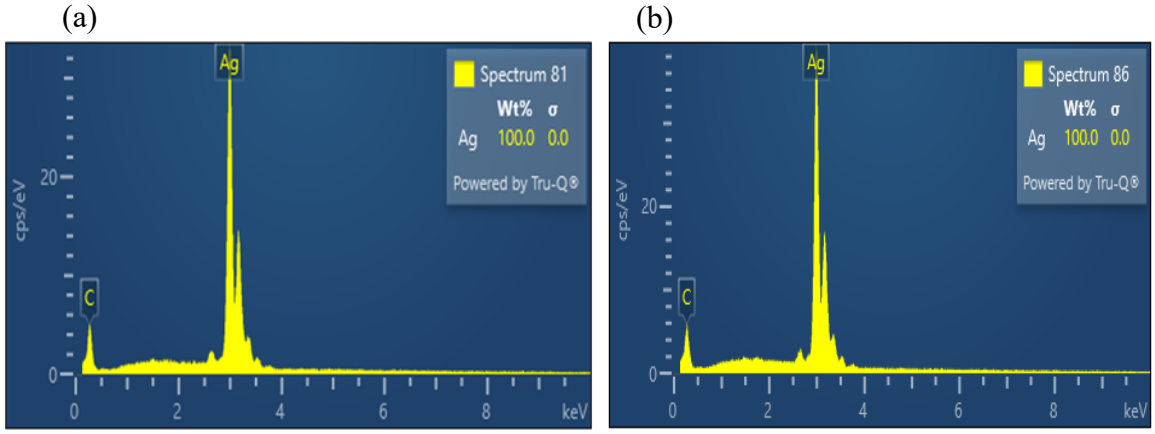

Figure 26: EDS analysis of silver (Ag) (only Ar) at (a) 600 °C, and (b) 700°C

The EDS spectrum shows only silver peaks, indicating 100% metallic Ag. This complete reduction occurs without hydrogen because silver nitrate decomposes to silver oxide and then metallic silver at elevated temperature, and once the first silver nuclei form, further reduction of residual Ag^+ proceeds via an autocatalytic deposition mechanism (Stern, 1972). In the hydrogen-assisted synthesis, hydrogen plays the role of the reductant and ensure rapid, complete conversion to metallic silver as well, so the decomposition in both cases in essentially pure Ag.

3.3 Comparison of Hydrogen and Argon atmospheres

EDS showed that silver nanoparticles formed under both hydrogen and argon atmosphere had similar purity, with only metallic Ag detected. The difference lies in the reaction kinetics that govern nucleation and growth. Under hydrogen, the strong reducing conditions slowed nucleation, creating fewer starting points. This allowed the particles to grow larger, but they became less uniform in size. In contrast, the inert argon atmosphere promoted more extensive nucleation during precursor decomposition, leading to a greater number of

smaller, more homogeneously distributed particles. Similar trends have been reported in the literature: Kondeti et al. (2017) showed that hydrogen plasmas accelerate reduction but do not necessarily enhance nucleation, while M. Darwish et al. (2022) observed that argon based processes can sustain nanoparticle formation without hydrogen, often yielding finer distributions. Together, these results confirm that the choice of gas atmosphere plays a decisive role in balancing nucleation and growth, with hydrogen favouring growth and argon favouring nucleation.

Table 9:Summary of Properties of Silver Nanoparticles in H_2 and Ar

Condition/Property	Hydrogen	No Hydrogen (only Ar)
Gas role	Strong reducing gas	Inert gas (no reduction)
Size at 600 °C	Large and less uniform	Mixed sizes, some agglomerates
Size at 700°C	Smaller and more uniform	Smaller and more uniform
Shape	Mostly spherical, smooth	Mostly spherical, smooth
Agglomeration	600 °C: slow 700°C: more compact	600 °C: some clusters 700°C: better packing
Purity	100% metallic silver	100% metallic silver
Main difference	Hydrogen changes nucleation, fewer but larger particles at lower temperature	Argon relies on heating only, smaller particles for same temperature

3.4 Copper powders produced via USP–HR

The synthesis of copper nanoparticles was visually evident through a distinct change in the

color of the precursor solution (Figure *27*). Initially, the solution exhibited a blue hue due to the presence of copper nitrate trihydrate. As the reaction progressed, the color gradually shifted to red, indicating the formation of metallic copper nanoparticles. This change is attributed to the surface plasmon resonance of the nanoparticles, which produces the characteristic red color. Thus, the color transition from blue to red served as a simple yet clear visual confirmation of successful synthesis.

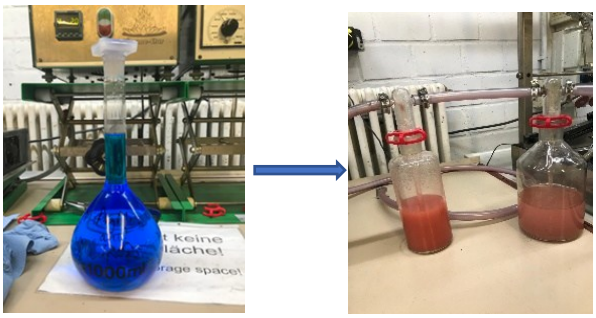

Figure 27:Solution color change during copper nanoparticles synthesis

3.4.1 Hydrogen reduction of copper nitrate trihydrate

The hydrogen assisted reduction of copper nitrate was carried out to investigate the influence of temperature on the phase transformation and morphology of the resulting copper powders. Copper nitrate trihydrate ($Cu(NO_3)_2 \cdot 3H_2O$) initially undergoes dehydration, followed by thermal decomposition to form copper oxide (CuO) (Morozov et al., 2003). In the presence of hydrogen, CuO is subsequently reduced to metallic copper (Kim et al., 2003) according to the following reactions:

$$Cu(NO_3)_2 \cdot 3H_2O \longrightarrow CuO + 2NO_2 + \frac{1}{2} O_2 + 3H_2O \qquad \text{(Eq. 11)}$$

$$CuO + H_2 \longrightarrow Cu + H_2O \qquad \text{(Eq. 12)}$$

The crystallization water in $Cu(NO_3)_2 \cdot 3H_2O$ facilitates the initial decomposition by promoting the formation of porous intermediate structures, enhancing gas–solid interactions between CuO and hydrogen. However, because copper has a lower standard reduction potential ($E° = +0.34$ V) than silver nitrate, the reduction of copper nitrate trihydrate proceeds more slowly. Therefore, to get total reduction, greater temperatures or longer hydrogen exposure are needed.

3.4.2 Temperature influence on morphology and composition of Cu NPs

Temperature has a major impact on the shape, elemental makeup, and purity of the produced copper particles in ultrasonic spray pyrolysis (USP). Figure *28*, displays SEM images magnified by 1 µm of particles produced with a 1 (M) copper nitrate precursor solution at 550 °C, 600 °C, 650 °C and 700 °C.

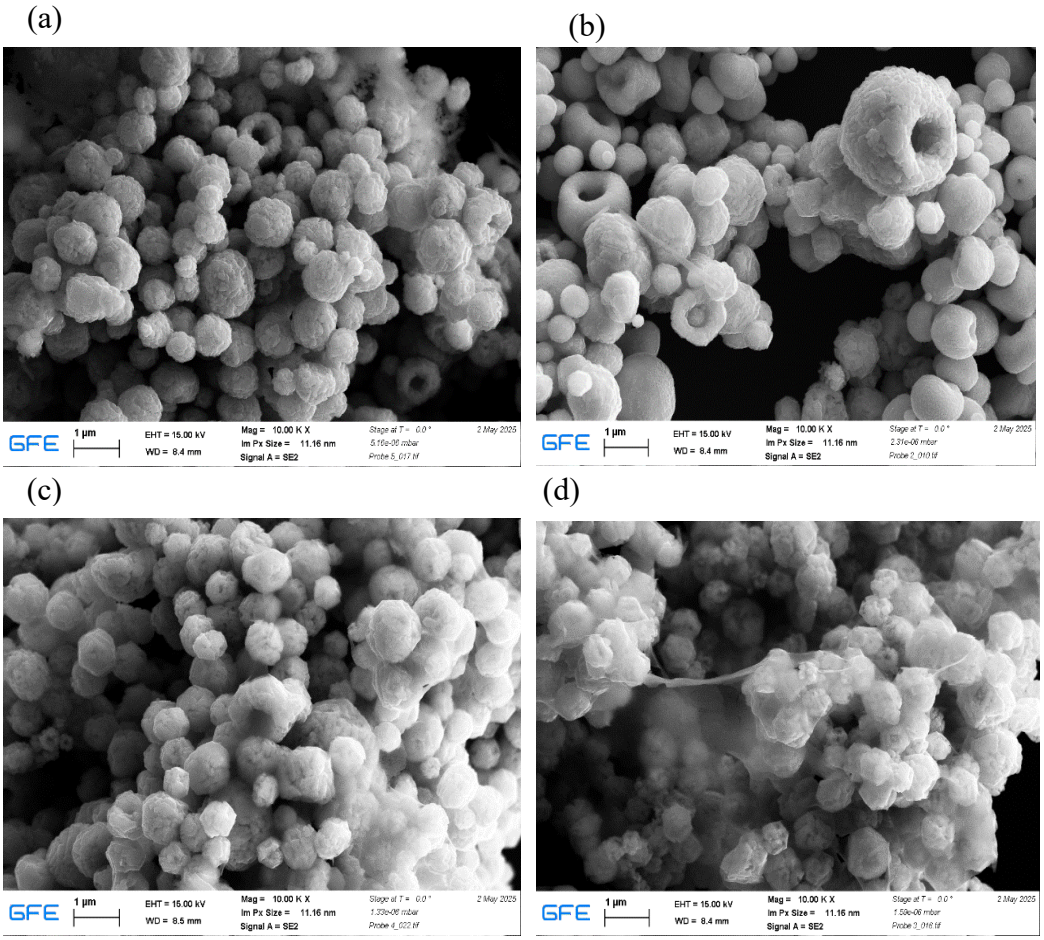

Figure 28: SEM analysis of Cu particles produced at 1 mol/L (a) 550 °C, (b) 600 °C, (c) 650 °C and (d) 700 °C

In terms of morphology, at 550 °C, the particles appeared as cauliflower like agglomerates, where growth and partial sintering dominated. This produced broad size distributions and many fused clusters. Under USP/H_2 conditions, rapid solvent evaporation and faster reduction at higher temperatures induced burst nucleation of numerous small nuclei within each droplet, limiting the time available for coalescence and leading to finer, more discrete particles. However, the degree of agglomeration also increased with temperature; it was mild at 550 °C but became severe at 700 °C, suggesting stronger interparticle interactions and enhanced sintering at elevated temperatures.

These observations align with previous research on copper nanoparticles synthesis, which reported an optimal range of 600-650°C for producing monodisperse nanoparticles, while higher temperatures tend to promote undesirable agglomeration (Harishchandra et al., 2020).

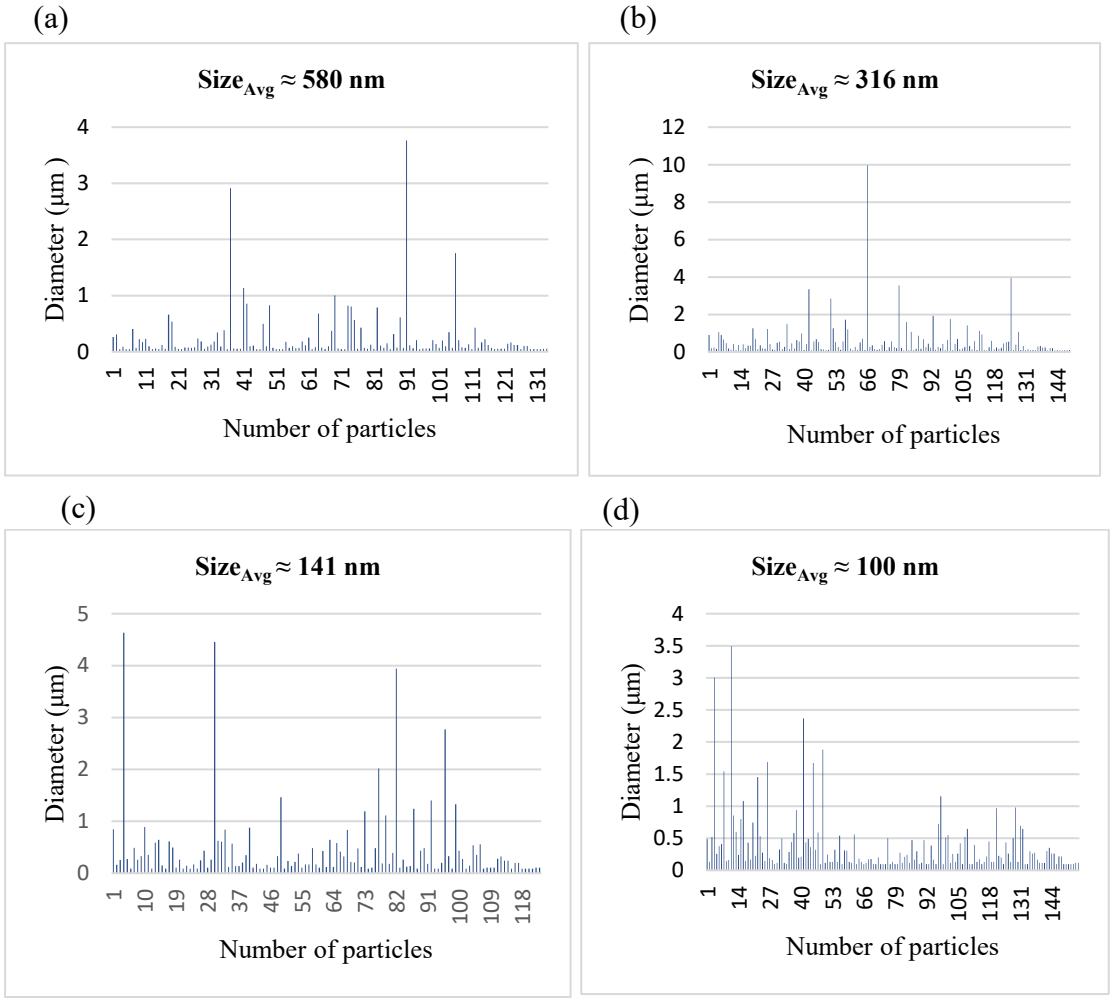

Figure 29: Average size of Cu nanomaterials at (a) 550 °C, (b) 600 °C, (c) 650 °C and (d) 700 °C

The synthesis also revealed that copper nanoparticles size and distribution are highly dependent on temperature. Average particle size decreased from about 580 nm at 550 °C to around 100 nm at 700 °C. Between 550 °C and 650 °C, the size reduction was accompanied by a narrowing of the distribution, indicating that higher temperatures promote faster nucleation and yield smaller, more homogeneous particles.

Based on the EDS results expressed as weight percent (wt.%), the copper content remained essentially constant across all investigated temperatures. Nonetheless, a discernible drop in oxygen content was noted with rising temperatures, suggesting enhanced reduction

effectiveness and a decrease in residual oxides at higher temperatures.

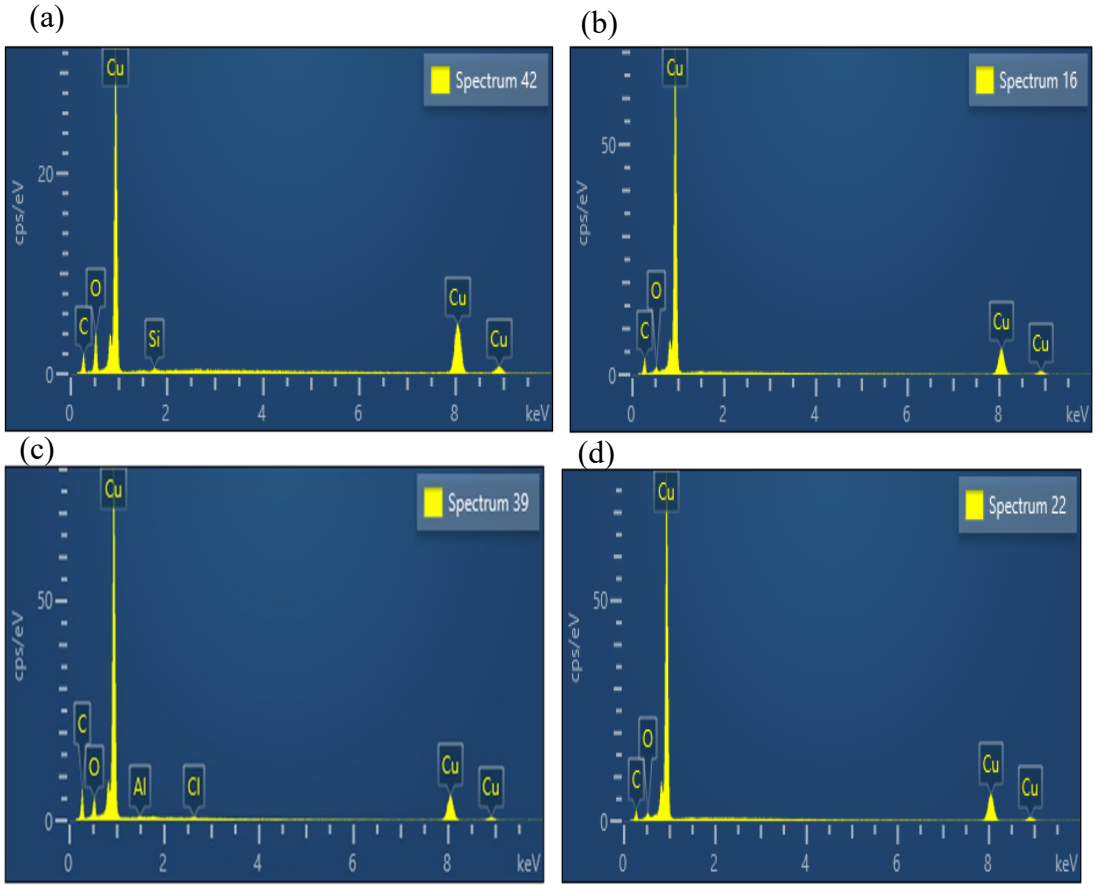

Figure 30: EDS spectrums for Cu particles at 1 mol/L (a) 550 °C, (b) 600 °C, (c) 650 °C and (d) 700 °C

Table 10:EDS results of Cu produced at different temperatures at 1 mol/L

Temperature (°C)	**Element (wt.)**				
	Cu	O	Cl	Si	Al
550	90.5	8.9	-	0.6	-
600	94.6	5.4	-	-	-
650	94.7	4.6	0.3	-	0.4
700	98.1	1.2	-	-	-

This trend suggests that higher temperatures promote a more thorough breakdown of the copper precursor and enhance reduction efficiency, thereby leading to purer metallic copper. Similar findings were reported by Luna et al. (2015) , where EDS analysis of copper

oxide nanoparticles annealed at 600 °C revealed ~91.3 wt.% Cu and ~8.7 wt.% O, confirming the strong correlation between temperature and metallic copper purity.

Depending on the synthesis temperature, the elemental analysis of the synthesized copper samples showed the presence of several elements, including Cu, O, Si, Cl, Al, and C. The silicon (Si) found at lower temperatures is the result of contamination from the silica tube used in the reactor system. It is possible that the chlorine (Cl) detected at temperatures above 600 °C originates from deionized water used during precursor and sample preparation that was not properly distilled and purified. The source of aluminium (Al) seen in EDS analysis at higher temperatures is contamination during the sample preparation or measurement procedure. Carbon (C), which is only detected at 600°C, might originate from the carrier gases or organic residues in the precursor solution. Higher copper purity and reduced oxygen content were generally the results of raising the synthesis temperature; 600 °C seems to be the most efficient temperature for producing high-purity Cu with little oxidation.

The observed trends in morphology, purity, and agglomeration at different temperatures also suggest potential application-specific advantages. At 600–650 °C, the particles were small, uniform, and pure, which makes them suitable for electronics applications such as conductive inks and printed circuits, where high conductivity is essential. At 700 °C, the particles were even smaller, which is useful for catalysis, since a large surface area improves catalytic activity, although the strong agglomeration at this temperature could limit performance. At the lower temperature of 550 °C, the cauliflower-like agglomerates, with their rough surfaces, could be useful for antimicrobial coatings, where surface reactivity is more important than conductivity. This shows that by controlling the synthesis temperature in USP–HR, it is possible to obtain copper nanoparticles with properties tailored for different applications.

3.5 Cu-Ag bimetallic particle generated by the USP-HR:

We start with a mixed solution containing amounts of copper nitrate trihydrate and silver nitrate. When this mixture is sprayed into the hot USP reactor and meets the hydrogen gas, the nitrates break down and are reduced to metals. Silver nitrate decomposes directly to metallic silver without forming stable oxide intermediates, while copper nitrate trihydrate first loses its waters of hydration, decomposes to copper oxide, and is subsequently reduced

by hydrogen to copper metal, producing water as a by-product.

If we sum these steps, two moles of $AgNO_3$ and one mole of $Cu(NO_3)_2 \cdot 3H_2O$ reacting with four moles of H_2 give the overall stoichiometric equation (Köroğlu et al., 2021):

$$2AgNO_3 + Cu(NO_3)_2 \cdot 3H_2O + 4H_2 \rightarrow 2Ag + Cu + 4NO_2 + 7H_2O \quad \text{(Eq. 13)}$$

3.5.1 Cu-Ag bimetallic particles (1:1 precursor ratio)

Cu-Ag particles were generated at 550 °C, 600 °C, 650 °C and 700 °C using 0.5 M of copper nitrate and 0.5 M of silver nitrate (1:1 Cu:Ag), with 1 L/min of H_2 and 1 L/min carrier gas flow (Ar) and the residence time was the same.

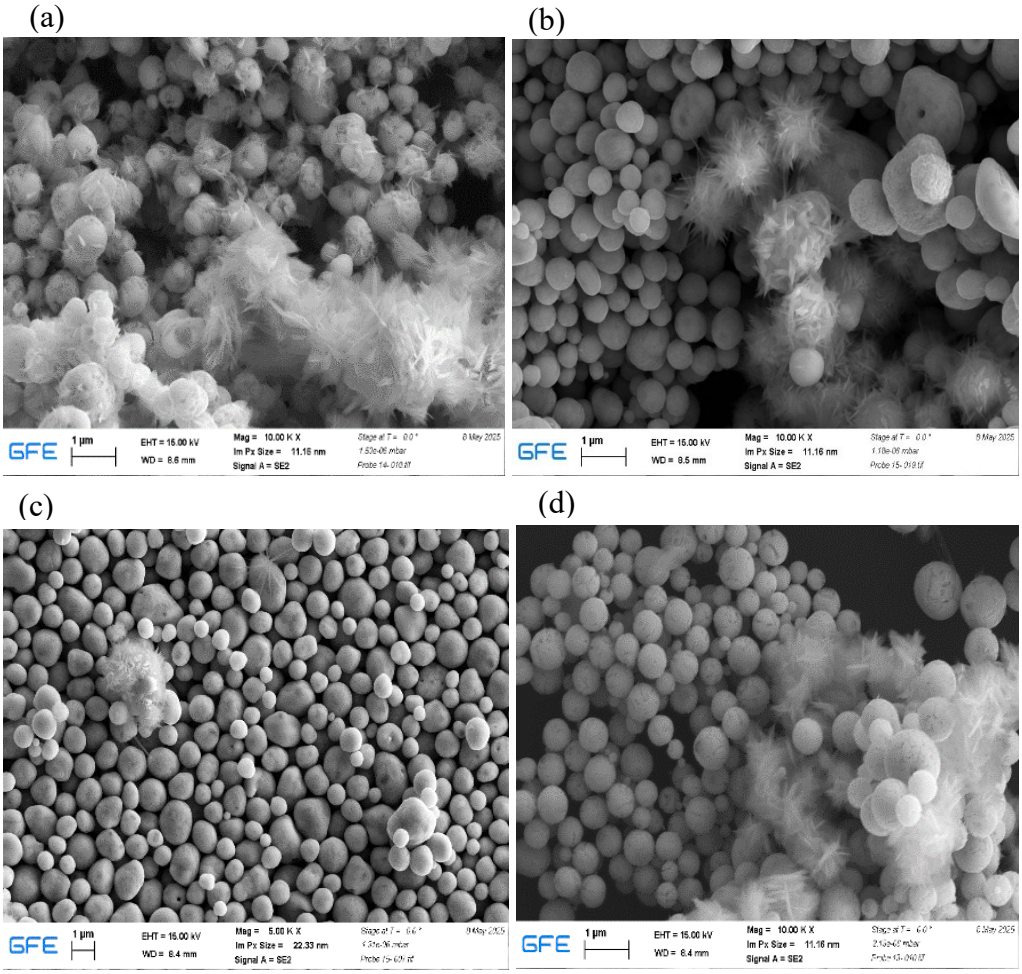

Figure 31: SEM images of Cu-Ag nanosized particles, (a) 550 °C, (b) 600 °C, (c) 650 °C and (d) 700 °C

SEM images show that at 550 °C most particles are spherical but covered with needle-like whiskers, giving them a fluffy appearance and indicating incomplete reduction or rapid local oxidation. At 600 °C, particles are predominantly spherical with smooth surfaces,

showing fewer surface irregularities compared to 550 °C. When the temperature is increased to 650 °C, the particles become more uniformly spherical with fewer whiskers. At 700 °C, sintering becomes pronounced. The SEM image reveals a mixture of large spheres and dendritic clusters; some particles have grown beyond 1 µm.

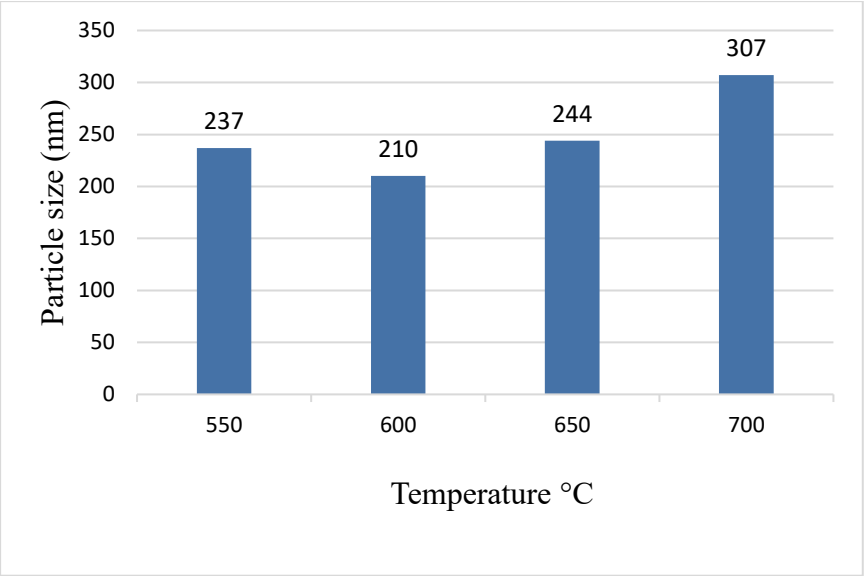

Figure 32: Effect of synthesis temperature on for Cu-Ag nanoparticles size

The particle size of Cu-Ag nanoparticles was strongly influenced by the synthesis temperature. At 550 °C, the particles exhibited an average area is 63 nm² with an average particle size of 237 nm. Increasing the temperature to 600 °C led to a reduction in average particle size (210 nm), and a narrower distribution indicating improved homogeneity. At 650 °C, the mean diameter increased to 244 nm suggesting partial densification of the particles. Finally At 700 °C, ImageJ analysis of 106 particles shows a mean ferret diameter of 307 nm and an average area of 62 nm².

Overall, the mean particle diameter increased from 237 nm at 550 °C to 307 nm at 700 °C, indicating that higher synthesis temperatures favor particle growth. This growth can be attributed to enhanced atomic diffusion and sintering at elevated temperatures, which promote particle coalescence and grain growth. As temperature rises, surface energy minimization drives smaller particles to merge into ones, resulting in an overall increase in particle size

EDS analysis confirms that the synthesized particles contain both Cu and Ag in nearly a 1:1 atomic ratio across all investigated samples. Minor oxygen peaks were detected,

suggesting traces of surface oxides, but these did not significantly alter the overall composition. The near stoichiometric Cu:Ag ratio indicates efficient co-reduction of both metal precursors during synthesis, leading to almost homogeneous bimetallic particles.

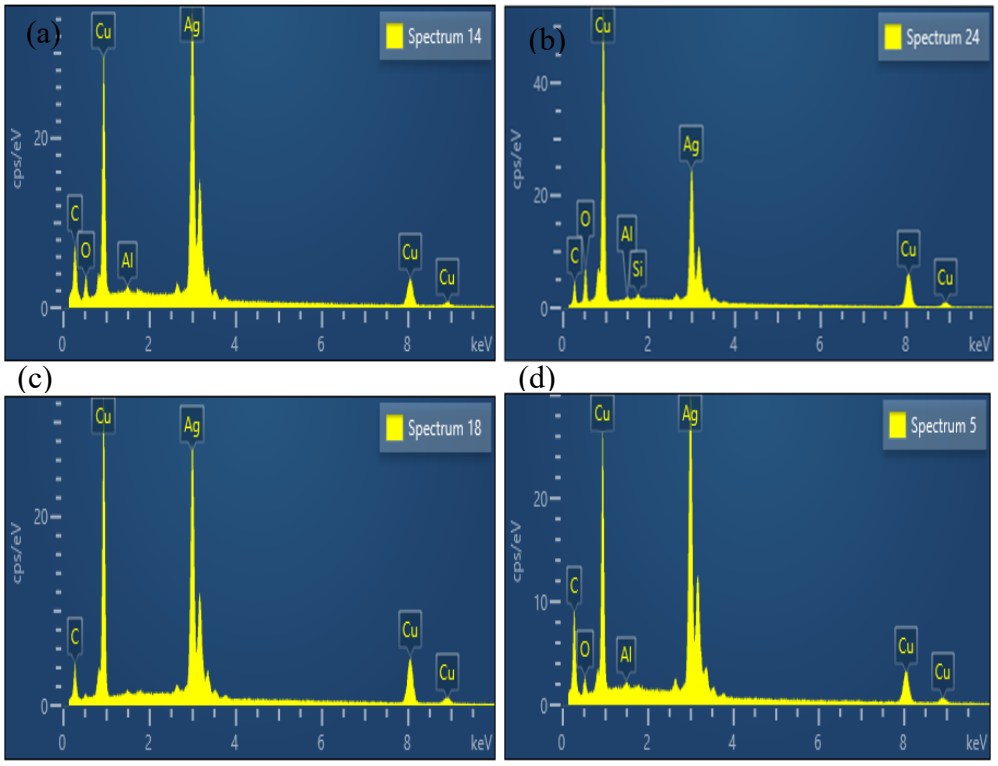

Figure 33: EDS analyses of Cu-Ag nanosized particles, (a) 550 °C, (b) 600 °C, (c) 650 °C and 700 °C

Table 11:Elemental composition of Cu-Ag (0.5 M both) at different temperature

Temperature °C	**Element (w %)**		
	Cu	**Ag**	**O**
550	59	37.7	3.9
600	53.2	39.9	6.3
650	54.8	45.2	-
700	59.1	37.7	2.9

According to (Yang et al., 2020) Copper and silver are immiscible at almost all compositions so hydrogen reduction of mixed nitrates tends to produce phase-segregated Cu-Ag core-shell particles than homogeneous alloys. And silver has a lower surface energy

and therefore migrates to the outer surface, while copper (with higher surface energy) forms the core.This behaviour is advantageous: a silver-rich shell shields the copper core from oxidation and provides noble-metal surface properties (Kim et al., 2021). In the present study, the EDS results show Cu:Ag ratios close to the intended 1:1 atomic ratio, confirming that the overall bimetallic composition is preserved. At 650 °C, the absence of oxygen peaks suggests complete reduction and may be consistent with the formation of a continuous Ag shell.

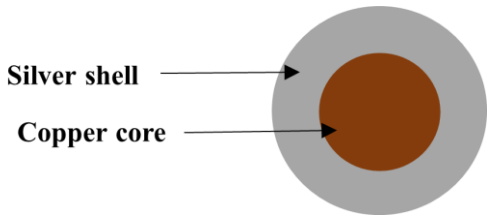

Figure 34: Representation of Cu-Ag core-shell

3.5.2 Cu-Ag bimetallic particles (1:3 precursor ratio)

To compare and analyze how the precursor ratio influences the characteristics of Cu@Ag bimetallic powders, we examined the sample prepared at 650 °C with a 1:3 Cu:Ag ratio and compared it with the 1:1 ratio sample. This temperature was chosen because for 1:1 ratio, no impurities were detected and the particles were generally more uniform.

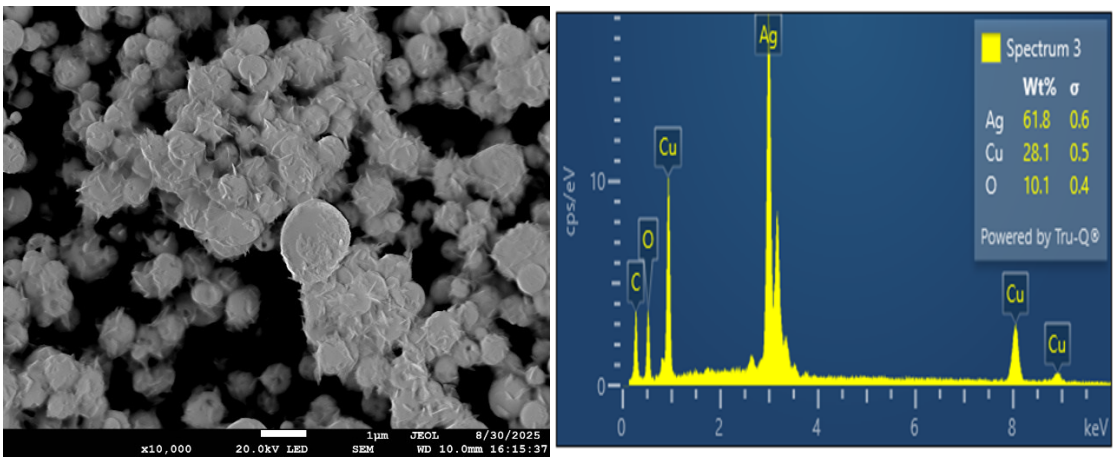

Figure 35: SEM and EDS results of 1:3 Cu:Ag NPs

The 1:3 powder shows a larger average particle size of 280 nm (from ImageJ) and more clustering, consistent with faster Ag nucleation and higher Ag surface mobility, which promote coalescence. Several particles display a rough surface and EDS reveals about 10 wt % oxygen, attributed to post-synthesis oxidation of exposed Cu during ~1 month of air

storage; this oxidation can roughen the surface and degrade electrical/thermal properties. In contrast, the 1:1 powder exhibits more uniform, spherical particles (244 nm) as shown in (Figure *32*), with only rare whiskers and no measurable oxygen, indicating complete reduction and better surface preservation at the time of analysis. These observations are consistent with Ag surface enrichment at 650 °C, with the Ag-rich (1:3) sample being more prone to clustering and, when stored in air, to localized oxidation at defects where Cu is exposed.

These findings suggest that the Cu:Ag ratio strongly influences the suitability of the powders for catalytic applications. The 1:1 sample, with its smaller, more uniform, and oxidation-free particles, offers a higher surface area and better stability, making it more promising for applications requiring long-term activity and reproducibility. In contrast, the 1:3 sample, while Ag-rich and potentially more selective for Ag-dominated reactions, shows clustering and surface oxidation, which may reduce accessible active sites and necessitate a pre-reduction step before use. Overall, tuning the Cu:Ag ratio provides a pathway to optimize surface area, stability, and surface composition for specific catalytic processes.

Partial Conclusion

This research shows that the synthesis conditions particularly gas atmosphere, temperature, and precursor ratio have a strong effect on the morphology, purity, and stability of the produced powders. The findings confirm that careful adjustment of these parameters allows tailoring particle size, surface state, and overall performance, making the materials suitable for applications in electronics, catalysis, and coatings.

GENERAL CONCLUSION AND PERSPECTIVE

General conclusion and perspectives

This thesis demonstrates that gas atmosphere, temperature, and precursor ratio significantly influence the morphology, purity, and surface state of Ag, Cu, and Cu–Ag powders synthesized via ultrasonic spray pyrolysis and hydrogen-assisted reduction. For Ag, hydrogen produced larger and less uniform particles, while argon promoted smaller and more homogeneous ones. For Cu, synthesis at 600–650 °C yielded small, pure, and uniform particles suitable for electronic applications, whereas 700 °C produced even smaller particles with stronger agglomeration, which could be useful for catalysis. For Cu–Ag, the 1:1 ratio resulted in smaller, more uniform, and oxidation-free particles, while the 1:3 ratio produced larger clustered particles with surface oxidation after storage. However, only a limited number of precursor ratios and temperatures were explored, which does not capture the full process window. Structural analysis relied mainly on SEM and EDS, while XRD was used in a limited way and did not fully explore phase evolution across all samples. More surface-sensitive methods such as XPS would also give deeper insights into oxidation states and surface chemistry. Functional properties such as conductivity or catalytic activity were not directly measured, so the link between structure and application remains indirect.

The research questions were answered. Cu, Ag, and Cu-Ag powders were successfully made in the 500-700 °C range, and their purity and particles shapes were compared under hydrogen and argon. The results showed that temperature controls particles size; medium temperatures gave uniform particles, but higher temperatures made smaller, more clumped ones. Hydrogen improved purity but did not always make uniform particles, while argon promoted more nucleation. And the 1:1 Cu-Ag ratio gave the best uniformity and oxidation resistance. This work provides useful insights by comparing mono- and bimetallic powders under controlled USP-HR conditions. It shows how process parameters can be adjusted to control particle size, shape, and stability. These results can guide the design of powders for applications such as electronics, catalysis, and coatings, and improve understanding of how bimetallic interactions affect growth and oxidation; helpful for both research and industry.

Future studies should explore a wider range of precursor ratios and temperatures to better understand how they affect structure and properties. Regular use of XRD is suggested to track phase formation, and advanced techniques like XPS or in-situ TEM could help study oxidation and core-shell formation in more detail. Testing storage under inert atmospheres

and using post-reduction treatments could improve powder stability. Finally, real performance tests, for example in conductive inks, catalysis, or coatings would confirm the practical usefulness of these powders.

BIBLIOGRAPHIC REFERENCES

Bang, J. H., & Suslick, K. S. (2010). Applications of ultrasound to the synthesis of nanostructured materials. Advanced Materials, 22(10), 1039–1059. https://doi.org/10.1002/adma.200904093

BHP. (2024). BHP Insights: how copper will shape our future. *Bhp*. Access on July 23, 2025, from https://www.bhp.com/news/bhp-insights/2024/09/how-copper-will-shape-our-future

Hanapin, S. E. (2023). *Comparisons of Silver Nanoparticle Synthesis Methods by Microwave and Non-Microwave using Hydrogen Gas as a Reducing Agent*. 4–5.

Hong, X., Zhu, H., Du, D., Zhang, Q., & Li, Y. (2023). Research Progress of Copper-Based Bimetallic Electrocatalytic Reduction of CO2. *Catalysts*, *13*(2). https://doi.org/10.3390/catal13020376

Hu, C., He, G., Yang, Y., Wang, N., Zhang, Y., Su, Y., Zhao, F., Wu, J., Wang, L., Lin, Y., & Shao, L. (2024). Nanomaterials Regulate Bacterial Quorum Sensing: Applications, Mechanisms, and Optimization Strategies. *Advanced Science*, *11*(15). https://doi.org/10.1002/advs.202306070

Islam, S. N., Naqvi, S. M. A., Parveen, S., & Ahmad, A. (2021). Application of mycogenic silver/silver oxide nanoparticles in electrochemical glucose sensing; alongside their catalytic and antimicrobial activity. *3 Biotech*, *11*(7), 1–11. https://doi.org/10.1007/s13205-021-02888-4

Kim, T. H., Kim, H., Jang, H. J., Lee, N., Nam, K. H., Chung, D. won, & Lee, S. (2021). Improvement of the thermal stability of dendritic silver-coated copper microparticles by surface modification based on molecular self-assembly. *Nano Convergence*, *8*(1). https://doi.org/10.1186/s40580-021-00265-8

Kim, J. Y., Rodriguez, J. A., Hanson, J. C., Frenkel, A. I., & Lee, P. L. (2003). Reduction of CuO and Cu_2O with H_2: H embedding and kinetic effects in the formation of suboxides. Journal of the American Chemical Society, 125(35), 10684–10692. https://doi.org/10.1021/ja0301673

Köroğlu, M., Ebin, B., Stopic, S., Gürmen, S., & Friedrich, B. (2021). One step production of silver-copper (Agcu) nanoparticles. *Metals*, *11*(9). https://doi.org/10.3390/met11091466

Kostić, D., Stopic, S., Keutmann, M., Emil-Kaya, E., Husovic, T. V., Perušić, M., &

Friedrich, B. (2024). Synthesis of Titanium-Based Powders from Titanium Oxy-Sulfate Using Ultrasonic Spray Pyrolysis Method. *Materials*, *17*(19). https://doi.org/10.3390/ma17194779

Larm, N. E., Stachurski, C. D., Trulove, P. C., Tang, X., Shen, Y., Durkin, D. P., & Baker, G. A. (2025). Role of Heavy Water in the Synthesis and Nanocatalytic Activity of Gold Nanoparticles. *ACS Nanoscience Au*, *5*(1), 52–59. https://doi.org/10.1021/acsnanoscienceau.4c00069

Lin, Z., Guo, M., & Zhang, X. (2024). Bimetallic nanoparticles: Structure, properties, and catalytic applications. Materials Chemistry Frontiers, 8(3), 540–555. https://doi.org/10.1039/D3QM01234A

Lu, L., & An, X. (2015). Silver nanoparticles synthesis using H2 as reducing agent in toluene-supercritical CO2 microemulsion. *Journal of Supercritical Fluids*, *99*, 29–37. https://doi.org/10.1016/j.supflu.2014.12.024

Magdassi, S. (2010). The chemistry of inkjet inks. World Scientific Publishing. https://doi.org/10.1142/7438

Majerič, P., & Rudolf, R. (2020). Advances in ultrasonic spray pyrolysis processing of noble metal nanoparticles-Review. *Materials*, *13*(16). https://doi.org/10.3390/MA13163485

Mallikarjuna, K., & Kim, H. (2018). Synthesis of shape and size-dependent CuAg bimetallic dumbbell structures for organic pollutant hydrogenation. *Physica E: Low-Dimensional Systems and Nanostructures*, *102*(April), 44–49. https://doi.org/10.1016/j.physe.2018.04.033

Mhetre, Mrs. H. V., Kanse, Dr. Y. K., & Patil, Dr. S. S. (2021). Nanomaterials: Applications in Electronics. *International Journal of Advanced Engineering and Nano Technology*, *4*(6), 7–19. https://doi.org/10.35940/ijaent.d0464.094621

Mondal, S. K., Chakraborty, S., Manna, S., & Mandal, S. M. (2024). Antimicrobial nanoparticles: current landscape and future challenges. *RSC Pharmaceutics*, *1*(3), 388–402. https://doi.org/10.1039/d4pm00032c

Morozov, I. V., Znamenkov, K. O., Korenev, Yu. M., & Shlyakhtin, O. A. (2003). Thermal decomposition of $Cu(NO_3)_2 \cdot 3H_2O$ at reduced pressures. Thermochimica Acta, 403(2), 173–179. DOI: 10.1016/S0040-6031(03)00057-1.

Oladipo, A. A., Oskouei, S. D., & Gazi, M. (2023). Metal-organic framework-based nanomaterials as opto-electrochemical sensors for the detection of antibiotics and

hormones: A review. *Beilstein Journal of Nanotechnology*, *14*, 631–673. https://doi.org/10.3762/bjnano.14.52

Rahemi Ardekani, S., Sabour Rouh Aghdam, A., Nazari, M., Bayat, A., Yazdani, E., & Saievar-Iranizad, E. (2019). A comprehensive review on ultrasonic spray pyrolysis technique: Mechanism, main parameters and applications in condensed matter. *Journal of Analytical and Applied Pyrolysis*, *141*(June), 104631. https://doi.org/10.1016/j.jaap.2019.104631

Rukini, A., Rhamdhani, M. A., Brooks, G. A., & Van den Bulck, A. (2022). Metals Production and Metal Oxides Reduction Using Hydrogen: A Review. *Journal of Sustainable Metallurgy*, *8*(1), 1–24. https://doi.org/10.1007/s40831-021-00486-5

Sahoo, J., Sarkhel, S., Mukherjee, N., & Jaiswal, A. (2022). Nanomaterial-Based Antimicrobial Coating for Biomedical Implants: New Age Solution for Biofilm-Associated Infections. *ACS Omega*, *7*(50), 45962–45980. https://doi.org/10.1021/acsomega.2c06211

Sharma, N., Ojha, H., Bharadwaj, A., Pathak, D. P., & Sharma, R. K. (2015). Preparation and catalytic applications of nanomaterials: a review. *RSC Advances*, *5*(66), 53381–53403. https://doi.org/10.1039/c5ra06778b

Singh, A., A. Chavan, V., P, A., Udaynadh, B., & Adithi, E. (2024). Nanomaterial Characterization Techniques. *Futuristic Trends in Chemical Material Sciences & Nano Technology Volume 3 Book 13*, *May*, 18–45. https://doi.org/10.58532/v3becs13p1ch2

Singh, V., Yadav, P., & Mishra, V. (2020). Recent advances on classification, properties, synthesis, and characterization of nanomaterials. *Green Synthesis of Nanomaterials for Bioenergy Applications*, *September*, 83–97. https://doi.org/10.1002/9781119576785.ch3

Stern, K. H. (1972). High Temperature Properties and Decomposition of Inorganic Salts, Part 3: Nitrates and Nitrites. Washington, D.C.: Naval Research Laboratory, Electrochemistry Branch.

Stopic, S., Hounsinou, A. H., Husovic, T. V., Emil-Kaya, E., & Friedrich, B. (2024). Synthesis of AgCoCuFeNi High Entropy Alloy Nanoparticles by Hydrogen Reduction-Assisted Ultrasonic Spray Pyrolysis. *ChemEngineering*, *8*(3). https://doi.org/10.3390/chemengineering8030063

Stopić, S., Kostić, D., Damjanović, V., Perušić, M., Filipović, R., Nikolić, N., & Friedrich,

B. (2025). Recovery of titanium and aluminum from secondary waste solutions via ultrasonic spray pyrolysis. Metals, 15(7), 701. https://doi.org/10.3390/met15070701

Tang, J., Chu, M. sheng, Li, F., Feng, C., Liu, Z. gen, & Zhou, Y. sheng. (2020). Development and progress on hydrogen metallurgy. *International Journal of Minerals, Metallurgy and Materials*, *27*(6), 713–723. https://doi.org/10.1007/s12613-020-2021-4

Velgosova, O., Mačák, L., Čižmárová, E., & Mára, V. (2022). Influence of Reagents on the Synthesis Process and Shape of Silver Nanoparticles. *Materials*, *15*(19). https://doi.org/10.3390/ma15196829

Wang, L., Hu, C., & Shao, L. (2017). The antimicrobial activity of nanoparticles: Present situation and prospects for the future. *International Journal of Nanomedicine*, *12*, 1227–1249. https://doi.org/10.2147/IJN.S121956

Xiong, Z. (2017). *Ag-Cu Bimetallic Nanoparticle Synthesis and Properties*. A thesis submitted in partial fulfilment of Engineering. U.S.A 1–171.

Yang, C., Ko, B. H., Hwang, S., Liu, Z., Yao, Y., Luc, W., Cui, M., Malkani, A. S., Li, T., Wang, X., Dai, J., Xu, B., Wang, G., Su, D., Jiao, F., & Hu, L. (2020). Overcoming immiscibility toward bimetallic catalyst library. *Science Advances*, *6*(17), 1–9. https://doi.org/10.1126/sciadv.aaz6844

Xu, Y., Li, H., Gao, Y., Liu, X., Zhao, Y., & Zhang, J. (2024). Advances in Ultrasonic Spray Pyrolysis for Metal and Alloy Nanoparticles: Mechanisms, Control Strategies, and Applications. Nanomaterials, 14(7), 1758. https://doi.org/10.3390/nano14071758